PROPAGATION OF TWO SIMPLE ACOUSTIC TRANSIENTS IN AN ISOVELOCITY LAYER WITH PERFECTLY-REFLECTING BOUNDARIES

ALAN CHARLES MILLER
and
GEORGE FREDERICK WENDT

[redacted]

PROPAGATION OF TWO SIMPLE ACOUSTIC TRANSIENTS IN AN ISOVELOCITY LAYER WITH PERFECTLY-REFLECTING BOUNDARIES

by

Alan Charles Miller
Lieutenant, United States Navy
B.S. Chemical Engineering, Iowa State College, 1959

and

George Frederick Wendt
Lieutenant, United States Navy
B.S.C.E., Ohio University, 1959

Submitted in partial fulfillment of the
requirements for the degree of

MASTER OF SCIENCE IN PHYSICS

from the

NAVAL POSTGRADUATE SCHOOL
June 1967

ABSTRACT

The propagation of simple acoustic transients in an isovelocity water layer was investigated for the purpose of studying a relationship between the propagation of transients in ducts and in layers. The Laplace transform method was used to obtain approximate solutions for the acoustic pressure, particle velocity, and particle displacement resulting from a step-function input in velocity and the particle velocity resulting from a gated sine-wave input in velocity. Computer programs were written to evaluate and graph the resulting waveforms. The waveforms resulting from step-function and gated sine-wave inputs in velocity were observed and compared with the predicted waveforms. With the use of Mylar transducers, good correlation was obtained in the region of validity of the theoretical solutions. It was found that previously published solutions for the propagation of transients in ducts became the leading terms of the associated solutions for the layer.

TABLE OF CONTENTS

LIST OF TABLES

LIST OF ILLUSTRATIONS

LIST OF SYMBOLS

a radius of source

c free field speed of sound in water

$c = c\left[1-\left(\frac{\omega_n}{\omega}\right)^2\right]^{1/2}$, group velocity for frequency ω in the nth mode

$c_p = c^2/c_g$, phase velocity for frequency ω in the nth mode

d depth of the isovelocity layer

n mode number

r, z, t cylindrical coordinates, assuming radial symmetry, and time

ω_n angular cut-off frequency for the nth mode

ρ density of water

$\Phi = \sum_n \Phi_n$, acoustic velocity potential

$p = -\rho \frac{\partial \Phi}{\partial t}$, acoustic pressure

$\vec{u} = \nabla \Phi$, particle velocity

$\Phi_n = Z_n(z)\,\phi_n(r,t)$, acoustic velocity potential for the nth mode

$Z_n(z)$, transverse function for the nth mode in the layer

$\phi_n(r,t)$, radial portion of velocity potential for the nth mode in the layer

p_n acoustic pressure for the nth mode

$\vec{u}_n$ particle velocity for the nth mode

$u_{rn} = \frac{\partial}{\partial r}\Phi_n = \frac{\partial}{\partial t}\xi_n$, radial component of particle velocity for the nth mode in the layer

ξ_n radial particle displacement for the nth mode

$v_{rn} = u_{rn}/Z_n(z)$, fragment of the radial particle-velocity for the nth mode in the layer

p_{rn} fragment of the acoustic pressure for the nth mode in the layer

ξ_{rn} fragment of radial particle displacement for the nth mode in the layer

$\phi_n(z,t) = \Phi_n / R_n(r)$ longitudinal portion of the velocity potential for the nth mode in the duct

$R_n(r)$ transverse function for the nth mode in the duct

$p_{zn} = p_n / R_n(r)$ fragment of acoustic pressure for the nth mode in the duct

$v_{zn} = u_{zn} / R_n(r)$ fragment of longitudinal particle velocity for the nth mode in the duct

$\xi_{zn} = \xi_n / R_n(r)$, fragment of longitudinal particle displacement for the nth mode in the duct

u_{zn} longitudinal particle velocity for the nth mode in the duct

$I_\nu(\mu)$ modified Bessel functions of the first kind

$J_\nu(\theta)$ Bessel functions for the first kind

$K_\nu(\mu)$ modified Bessel functions of the third kind

$U_\nu(w\pm, ARG)$ Lommel functions of two variables

$ARG = \theta = \omega_n\sqrt{t^2 - T^2}$, argument of Bessel functions

$\mu = \frac{r}{c}\sqrt{s^2 + \omega_n^2}$, argument of modified Bessel functions

$T = \frac{r-a}{c}$, time of flight of signal from source at r=a to receiver in layer

$= z/c$, time of flight of signal from source at z=0 to receiver in duct

$t' = t - T$ delayed time which represents the elapsed time since a signal traveling with velocity c first arrived at position r in the layer or z in the duct

$V_a(t) = v_{rn}(a,t)$, velocity input at r=a in the layer

$V_o(t) = v_{zn}(0,t)$, velocity input at z=0 in the duct

$\phi_o(t) = \phi_n(0,t)$, pressure boundary condition at z=0 in the duct

$$1(z) = \left.\begin{array}{l} 0 \text{ for } z < 0 \\ 1 \text{ for } z > 0 \end{array}\right\} \text{unit step function}$$

γ	relative phase of layer solutions with respect to corresponding duct solutions
τ_m	values of t' for which $\xi_{rn} = 0$ in the layer
τ_{om}	values of t' for which $\xi_{zn} = 0$ in the duct
A	area of transducer face
C_o	blocked capacitance of transducer
C_s	compliance of transducer
e	input voltage to transducer
E_o	polarization voltage of transducer
R_s	source resistance in transmitter circuit
R_l	load resistance in the receiver circuit
x_o	equilibrium spacing between transducer film and back plate with polarizing voltage applied
β	transducer electro-mechanical transfer function

ACKNOWLEDGEMENTS

The continuing advice and assistance of Professor Alan B. Coppens of the Naval Postgraduate School is gratefully acknowledged.

Thanks are also due to Mr. Ernest G. Janzen for his assistance in the preparation of the computer programs.

This research was supported in part by the Naval Ships Systems Command.

1. INTRODUCTION

While most investigations of the propagation of energy in waveguides have been done for electromagnetic cases, some have considered the propagation of pulses of acoustical energy in waveguides[1,2,3,4]. The dispersion of an ultrasonic pulse propagated through a waveguide of circular cross-section filled with water has been used for the approximate determination of the frequency spectrum of the original pulse[1]. It has been shown that the dispersion of a rectangular pulse along an acoustic waveguide of rectangular cross-section can be used to calibrate the waveguide so it can be used to predict the effects of similar dispersion on the transmission of pulses of other shapes that are not amenable to actual computation[2]. Pulse-compression studies in an acoustic waveguide show that a frequency modulated input pulse can be compressed into an output pulse of shorter duration and of higher peak-amplitude[3]. In addition to the waveguide experiments, investigations of transients in layered media have been made[5,6]. W. C. Knudsen[5] investigated the propagation of a pressure transient in a surface layer of liquid which lay over a deep bottom layer of liquid. Many of these studies have used approximation techniques such as the method of stationary phase. A summary of these techniques useful for calculating the resultant propagated waveform has been presented by

J. R. Wait[7]. The original work of Rayleigh on scattering and radiation of harmonic disturbances by small cylinders was extended to transient disturbances by J. W. Miles using the Laplace transform[8]. R. B. Barakat used the Laplace transform to investigate the radiation of acoustic pulses of various shapes from an infinitely long circular cylinder[9].

Recently, exact solutions for the propagation of simple transients in waveguides (step-function and gated sine-wave inputs) have been published[4,10,11]. Some work has also been done which suggests a correlation between these exact solutions in ducts and solutions for the propagation of acoustic transients in isovelocity layers[12].

The purpose of this research is to investigate the region of validity of the suggested correlation and to see what, if any, restrictions must be placed on the resulting solutions describing the transient response of the layer. To facilitate this comparison, those results of the propagation of transients in ducts[4,12] which will be of value are summarized in Appendix A.

2. THEORY

Development of Solutions

The response of an isovelocity layer to simple transient excitations will be developed using the following assumptions:

(a) Cylindrical velocity-source of radius a.

(b) Constant layer depth, d.

(c) Perfectly-Reflecting upper and lower boundaries.

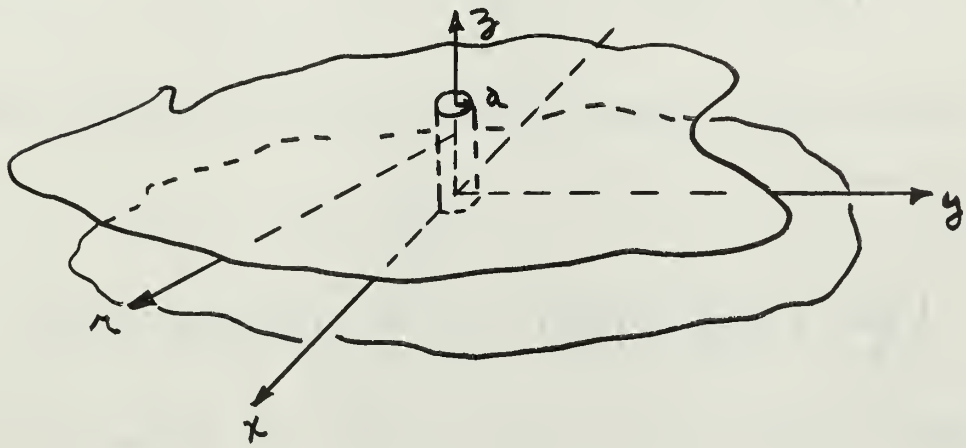

An Isovelocity Layer

Figure 2.1

For radially-symmetric propagation in the layer indicated in Figure 2.1, the wave equation for the acoustic velocity potential Φ can be written in cylindrical coordinates as

$$\left(\frac{\partial^2}{\partial r^2} + \frac{1}{r}\frac{\partial}{\partial r} + \frac{\partial^2}{\partial z^2} - \frac{1}{c^2}\frac{\partial^2}{\partial t^2}\right)\Phi(z,r,t) = 0 \qquad (2.1)$$

where r is the radial direction and z is the transverse direction.

The separation of variables

$$\Phi(z,r,t) = \sum_n \Phi_n(z,r,t) = \sum_n Z_n(z)\, \phi_n(r,t) \qquad (2.2)$$

leads to two partial differencial equations: one for a "transverse" function Z_n which depends only on the height z of the layer

$$\left[\frac{\partial^2}{\partial z^2} - \left(\frac{\omega_n}{c}\right)^2\right] Z_n(z) = 0 \,, \qquad (2.3)$$

and one for a "radial" portion ϕ_n of the acoustic velocity potential,

$$\left[\frac{\partial^2}{\partial r^2} + \frac{1}{r}\frac{\partial}{\partial r} - \left(\frac{\omega_n}{c}\right)^2 - \frac{1}{c^2}\frac{\partial^2}{\partial t^2}\right]\phi_n(r,t) = 0 \qquad (2.4)$$

which depends on both time, t, and the distance from the origin, r. The value of the separation constant ω_n depends on the nature of the boundaries at z = 0 and d. For example, if we have a pressure-release top and bottom, then $p = -\rho \frac{\partial \Phi}{\partial t} = 0$ at z = 0 and d and Eq. 2.3 has the solution

$$Z_n(z) = D \sin \frac{\omega_n}{c} z \qquad (2.5)$$

where $\omega_n = n\pi c/d$. Furthermore, since the source is assumed symmetric with respect to the plane z = d/2, just those modes having pressure antinodes at d/2 will be excited.

Thus only odd values of n are allowed. Therefore Eq. 2.5 can be rewritten as

$$Z_n(z) = D \sin\left(\frac{n\pi z}{d}\right), \quad n = 1, 3, 5, \text{etc.} \tag{2.6}$$

Since this transverse function affects the form of Eq. 2.4 only through the allowed values of ω_n, it is convenient to establish a set of reduced acoustic variables which suppresses the function $Z_n(z)$.

The well-known acoustic relations

$$p_n = -\rho \frac{\partial \Phi_n}{\partial t}, \tag{2.7a}$$

$$\vec{u}_n = \nabla \Phi_n, \tag{2.7b}$$

and

$$u_{rn} = \frac{\partial}{\partial r} \Phi_n \tag{2.7c}$$

where n is the mode number, p_n the acoustic pressure for the nth mode, $\vec{u}_n$ the particle velocity for the nth mode, and u_{rn} the radial particle velocity for the nth mode can be used with Eq. 2.2 to show that

$$p_n = -\rho\, Z_n(z) \frac{\partial}{\partial t} \phi_n(r,t). \tag{2.8}$$

The "fragment" p_{rn} of the acoustic pressure for the nth mode is defined as

$$p_{rn} \equiv p_n / Z_n(z) = -\rho \frac{\partial \phi_n}{\partial t} \qquad (2.9)$$

where $\phi_n = \phi_n\,(r,t)$ is the radial portion of the velocity potential for the nth mode which was previously defined by Eq. 2.2. Combination of Eqs.2.2 and 2.7c allows the definition of the "fragment" of the radial particle-velocity for the nth mode,

$$v_{rn} \equiv u_{rn} / Z_n(z) = \frac{\partial}{\partial r} \phi_n \,. \qquad (2.10)$$

Since the transverse function $Z_n\,(z)$ is independent of time, the radial particle-displacement for the nth mode may be obtained by integration of u_{rn} with respect to time. This enables the "fragment" of the radial particle-displacement for the nth mode to be written as

$$\xi_{rn} \equiv \xi_n / Z_n(z) = \frac{1}{Z_n(z)} \int_0^t u_{rn}\, dt \qquad (2.11)$$

These reduced acoustic variables or "fragments" ϕ_n, v_{rn}, p_{rn}, and ξ_{rn} will be used throughout the remainder of this development.

Since we are considering the propagation of transients, Eq. 2.4, a differential equation in two unknowns, cannot be solved by separation of variables. The Laplace transform method will be used to obtain the desired solutions.

The Laplace transform of Eq. 2.4 with quiescent initial conditions results in a differential equation in one unknown which may be written as

$$\left[\frac{\partial^2}{\partial r^2} + \frac{1}{r}\frac{\partial}{\partial r} - \left(\frac{\omega_n^2}{c} + s^2\right)\right]\bar{\phi}_n = 0 \tag{2.12}$$

where the bar over the function denotes the Laplace transform of that function:

$$\bar{\phi}_n(r,s) = \mathcal{L}\left\{\phi_n(r,t)\right\} = \int_0^{\infty} e^{-st}\,\phi_n(r,t)\,dt.$$

The change of variable

$$\mu = \frac{r}{c}\sqrt{s^2+\omega_n^2} \tag{2.13}$$

casts Eq. 2.12 into the form

$$\frac{\partial^2 \bar{\phi}_n}{\partial \mu^2} + \frac{1}{\mu}\frac{\partial \bar{\phi}_n}{\partial \mu} - \bar{\phi}_n = 0. \tag{2.14}$$

The solutions to Eq. 2.8 are $I_o(\mu)$ and $K_o(\mu)$, the modified Bessel functions of the first and third kind[13]. Conservation of energy requires $\bar{\phi}_n$ to go to zero as $s \rightarrow \infty$,

so that the only acceptable solution of this differential equation is $K_o\ (\mu)$. The Laplace transform of ϕ_n can now be expressed as

$$\bar{\phi}_n = C' K_o(\mu) \tag{2.15}$$

where C' is an amplitude constant to be determined from the boundary conditions.

With the use of the relationship expressed by Eq. 2.7c, the Laplace transform of v_{rn} becomes

$$\bar{v}_{rn} = \frac{\partial \bar{\phi}_n}{\partial r} = C' \frac{\partial K_o(\mu)}{\partial \mu} \frac{\partial \mu}{\partial r} = -\frac{C' \sqrt{s^2 + \omega_n^2}}{c} \tag{2.16}$$

The known boundary condition at the source, located at r = a, for propagation in the nth normal mode,

$$v_{rn}(a,t) = \frac{\partial \phi_n(a,t)}{\partial r} \equiv V_a(t), \tag{2.17}$$

has the transform

$$\bar{v}_{rn}(a,t) = \bar{V}_a\ . \tag{2.18}$$

Equations 2.16 and 2.18 allow evaluation of C',

$$C' = \frac{-\bar{V}_a c}{\sqrt{s^2+\omega_n^2}\; K_1\left(\frac{a}{c}\sqrt{s^2+\omega_n^2}\right)} \;, \tag{2.19}$$

so that $\bar{v}_{rn}$ can be expressed as

$$\bar{v}_{rn} = \bar{V}_a \; \frac{K_1\left(\frac{r}{c}\sqrt{s^2+\omega_n^2}\right)}{K_1\left(\frac{a}{c}\sqrt{s^2+\omega_n^2}\right)} \;. \tag{2.20}$$

The substitution for C' in Eq. 2.15 allows $\bar{\phi}_n$ to be written as

$$\bar{\phi}_n = \frac{-\bar{V}_a c \quad K_0\left(\frac{r}{c}\sqrt{s^2+\omega_n^2}\right)}{\sqrt{s^2+\omega_n^2} \quad K_1\left(\frac{a}{c}\sqrt{s^2+\omega_n^2}\right)} \;. \tag{2.21}$$

The expression for the Laplace transform of the fragment of acoustic pressure, $\bar{p}_{rn}$, can be obtained from Eq. 2.21 if we recall that $p_{rn} = -\rho \frac{\partial \phi_n}{\partial t}$ corresponds to $\bar{p}_{rn} = -\rho s \bar{\phi}_n$ in the transform domain. Thus,

$$\bar{p}_{rn} = \frac{\rho c s \bar{V}_a \;\; K_0\left(\frac{r}{c}\sqrt{s^2+\omega_n^2}\right)}{\sqrt{s^2+\omega_n^2}\; K_1\left(\frac{a}{c}\sqrt{s^2+\omega_n^2}\right)} \;. \tag{2.22}$$

The Laplace transform of the particle-displacement fragment, $\bar{\xi}_{rn}$, can be obtained from $\bar{v}_{rn}$ by either integration with respect to t in the time domain or multiplication by 1/s in the transform domain. The result is:

$$\bar{\xi}_{rn} = \frac{\bar{V}_a}{s} \frac{K_1\left(\frac{r}{c}\sqrt{s^2+\omega_n^2}\right)}{K_1\left(\frac{a}{c}\sqrt{s^2+\omega_n^2}\right)} . \tag{2.23}$$

Inverse transforms of Eq. 2.20 - 2.23 have not been tabulated, so approximation methods must be used.

If μ (Eq. 2.13) is greater than unity the asymptotic form

$$K_\nu(\mu) \doteq \sqrt{\frac{2}{\pi\mu}}\, e^{-\mu}\left(1 + \frac{4\nu^2-1}{8\mu} + ---\right) \tag{2.24}$$

may be used[12,13]. The requirement $\mu > 1$ can be satisfied by restricting $c/a\omega_n$ to values less than unity. Substitution of Eq. 2.24 into Eq. 2.20 yields

$$\bar{v}_{rn} = \frac{\bar{V}_a \sqrt{\frac{\pi}{2r/c\sqrt{s^2+\omega_n^2}}}\, \exp\left[-\frac{r}{c}\sqrt{s^2+\omega_n^2}\right]\left(1+\frac{3}{8\frac{r}{c}\sqrt{s^2+\omega_n^2}}\right)}{\sqrt{\frac{\pi}{2\frac{a}{c}\sqrt{s^2+\omega_n^2}}}\, \exp\left[-\frac{a}{c}\sqrt{s^2+\omega_n^2}\right]\left(1+\frac{3}{8\frac{a}{c}\sqrt{s^2+\omega_n^2}}\right)} \tag{2.25}$$

which simplifies to

$$\bar{v}_{rn} = \frac{\bar{V}_a \sqrt{\frac{a}{r}}\; \exp\left[-T\sqrt{s^2+\omega_n^2}\right] \left[1 + \frac{3}{8\frac{r}{c}\sqrt{s^2+\omega_n^2}}\right]}{\left[1 + \frac{3}{8\frac{a}{c}\sqrt{s^2+\omega_n^2}}\right]} \tag{2.26}$$

where T = $\frac{r-a}{c}$ is the time-of-flight of the signal from source to receiver. Since $c/a\omega_n$ is restricted to values less than unity, the denominator can be expressed as

$$\frac{1}{\left(1 + \frac{3}{8\frac{a}{c}\sqrt{s^2+\omega_n^2}}\right)} \doteq 1 - \frac{3}{8\frac{a}{c}\sqrt{s^2+\omega_n^2}} \;, \tag{2.27}$$

so that we have

$$\bar{v}_{rn} = \bar{V}_a \sqrt{\frac{a}{r}}\; \exp\left[-T\sqrt{s^2+\omega_n^2}\right] \left[1 + \frac{3}{8\frac{r}{c}\sqrt{s^2+\omega_n^2}}\right] \left[1 - \frac{3}{8\frac{a}{c}\sqrt{s^2+\omega_n^2}}\right] \tag{2.28}$$

which simplifies to

$$\sqrt{\frac{r}{a}}\, \bar{v}_{rn} = \bar{V}_a \exp\left[-T\sqrt{s^2+\omega_n^2}\right] - \frac{\bar{V}_a\, 3c}{8a\sqrt{s^2+\omega_n^2}} \left(1 - \frac{a}{r}\right) \exp\left[-T\sqrt{s^2+\omega_n^2}\right] \tag{2.29}$$

where terms of order $(c/a\omega_n)^2$ have been dropped.

With similar manipulations the other desired acoustic variables can be obtained from Eqs. 2.21 - 2.23:

$$\sqrt{\frac{r}{a}}\,\bar{\phi}_n = \frac{-\bar{V}_a c}{\sqrt{s^2+\omega_n^2}} \exp\left[-T\sqrt{s^2+\omega_n^2}\right] + \frac{\bar{V}_a\, 3c^2}{8a\sqrt{s^2+\omega_n^2}}\left(1+\frac{a}{3r}\right) \exp\left[-T\sqrt{s^2+\omega_n^2}\right] \qquad (2.30)$$

$$\sqrt{\frac{r}{a}}\,\bar{p}_{rn} = \frac{\rho s \bar{V}_a}{\sqrt{s^2+\omega_n^2}} \exp\left[-T\sqrt{s^2+\omega_n^2}\right] - \frac{3\rho c^2 s \bar{V}_a}{8a(s^2+\omega_n^2)}\left(1+\frac{a}{3r}\right) \exp\left[-T\sqrt{s^2+\omega_n^2}\right] \qquad (2.31)$$

$$\sqrt{\frac{r}{a}}\,\bar{\xi}_{rn} = \frac{\bar{V}_a}{s} \exp\left[-T\sqrt{s^2+\omega_n^2}\right] - \frac{\bar{V}_a\, 3c}{8a\sqrt{s^2+\omega_n^2}}\left(1-\frac{a}{r}\right) \exp\left[-T\sqrt{s^2+\omega_n^2}\right] \qquad (2.32)$$

Equations 2.29 - 2.32 approximate the Laplace transforms of the desired acoustic variables for the boundary condition $V_a(t)$ at $r = a$ with the restriction $c/a\omega_n < 1$.

Comparison of Eq. 2.29 with Eqs. A.7 and A.9 shows that the terms of Eq. 2.29 have known inversions. For a step input, for which $\bar{V}_a = {}^1/_S$ the inverse transform for the fragment of the radial particle-velocity can be written down directly from the known results of the duct (see Appendix A.

$$\sqrt{\frac{r}{a}}\,v_{rn} = J_0(\mathrm{ARG}) + 2\sum_{m=1}^{\infty}\left(\frac{t-T}{t+T}\right)^{m} J_{2m}(\mathrm{ARG}) - \frac{3c}{8a\omega_n}\left(1-\frac{a}{r}\right) 2\sum_{m=1}^{\infty}\left(\frac{t-T}{t+T}\right)^{\frac{2m-1}{2}} J_{2m-1}(\mathrm{ARG}) \qquad (2.33)$$

where ARG $= \omega_n \sqrt{t^2 - T^2}$ and it is always understood that all solutions vanish for $t < T$.

The inverse transforms of the other acoustic quantities can be found similarly by using the known transform pairs from the duct case and the additional transform pairs developed in Appendix A. The results are

$$\sqrt{\frac{r}{a}}\,\phi_n = -\frac{c}{\omega_n}\left[2\sum_{m=1}^{\infty}\left(\frac{t-T}{t+T}\right)^{\frac{2m-1}{2}} J_{2m-1}(\text{ARG}) - \frac{3c}{8a\omega_n}\left(1+\frac{a}{3r}\right)4\sum_{m=1}^{\infty}\left(\frac{t-T}{t+T}\right)^{2m-1} J_{2(2m-1)}(\text{ARG})\right] \quad (2.34)$$

$$\sqrt{\frac{r}{a}}\,p_{rn} = \rho c\left[J_0(\text{ARG}) - \frac{3c}{8a\omega_n}\left(1+\frac{a}{3r}\right)2\sum_{m=1}^{\infty}(-1)^{m-1}\left(\frac{t-T}{t+T}\right)^{\frac{2m-1}{2}} J_{2m-1}(\text{ARG})\right] \quad (2.35)$$

$$\sqrt{\frac{r}{a}}\,\xi_{rn} = \frac{2}{\omega_n}\left[\sum_{m=1}^{\infty}(2m-1)\left(\frac{t-T}{t+T}\right)^{\frac{2m-1}{2}} J_{2m-1}(\text{ARG}) - \frac{3c}{8a\omega_n}\left(1-\frac{a}{r}\right)2\sum_{m=1}^{\infty} m\left(\frac{t-T}{t+T}\right)^{m} J_{2m}(\text{ARG})\right] \quad (2.36)$$

The quantity $t' = t - T$ appearing in Eqs. 2.33 - 2.36 and in ARG as $(t - T)(t + T) = t^2 - T^2$ represents the time which has elapsed since the signal traveling with velocity c first arrived at the position r. It will be referred to as the delayed time.

Equations 2.33 - 2.36 are the solutions for the transient

response of an isovelocity layer to a step input in velocity at r = a and t = 0.

Similar procedures may be used to obtain the fragment of the radial particle-velocity for a gated sine-wave input in velocity for which $\overline{V}_a = \frac{\omega}{s^2+\omega^2}$.

$$\sqrt{\frac{r}{a}}\, v_{rn} = U_1(v_+, ARG) + U_1(v_-, ARG) + \frac{3c_p}{8a\omega_n}\left(1-\frac{a}{r}\right)\left[U_0(v_+, ARG) - U_0(v_-, ARG)\right] \quad (2.37)$$

where $U_\nu(v_\pm, ARG)$ = Lommel function of two arguments[14,15].

$$U_\nu(v_\pm, ARG) = \sum_{m=0}^{\infty} (-1)^m \left(\frac{v_\pm}{ARG}\right)^{\nu+2m} J_{\nu+2m}(ARG)$$

and $\quad v_\pm = \omega(t-T)(1 \pm c_g/c)$.

Other acoustic quantities could not be completely solved in this case. Details are shown in Section A-3 of Appendix A.

Comparison of the above solutions with the solutions for the duct listed in Appendix A shows that in all cases the solutions previously obtained for the duct become the leading terms in the solutions developed for the layer.

A physical understanding of this can be gained by comparing propagation processes in a duct with those in a layer. While a duct presents a constant cross-section to

the propagating wave form for all time, a transient propagating outward in a layer is presented with an effective cross-sectional area which increases as r. However, for sufficiently large r the cross-sectional area will not change appreciably as the waveform propagates through unit distance. In the limit, therefore, we expect the radial divergence contained by the term $\frac{1}{r}\frac{\partial}{\partial r}$ in Eq. 2.4 to become insignificant. In this limit, propagation processes can be described by an equation virtually the same as Eq. A3 which describes propagation in a duct.

For this reason it is not surprising that the solutions for the duct become the leading terms of the layer solutions. The remaining terms in the layer solutions are correction terms necessitated by the fact that the layer does not actually present a constant cross-section to the propagating wave form.

The solutions for the transient response of an isovelocity layer have been developed with the restriction $c/a\omega_n < 1$. Since the cutoff frequency is given by $\omega_n = n\pi c/d$, this restriction places a limit on the relation between the depth of the layer and the size of the source, $d/a > n\pi$. If it is desired to remove this restriction a different expansion of the $K_{\nu}(\mu)$'s involved must be used.

Investigation of Solutions

The solutions developed for the layer have been obtained for a single mode. In determining the contributions to the solutions from other modes, attention must be given to the transverse behavior of the transmitted and received signals. The boundary condition on velocity at the source at r = a says that $V_a(t)$ vanishes for $z < 0$ and $z > d$ and is constant for $0 < z < d$. This condition can be met by representing $V_a(t)$ by a spatial Fourier-superposition of $[u(z) - u(z-d)]$ in terms of the normal modes across the face of the source:

$$V_a(t) = \frac{4}{\pi} \sum_{n=1}^{\infty} \left(\frac{1}{2n-1}\right) \sin \frac{(2n-1)\pi z}{d} \quad . \tag{2.38}$$

Notice that the higher modes contribute as $\frac{1}{2n-1}$ for this input. These higher modes have positive and negative portions in their waveforms over the depth of the layer. These positive and negative portions will partially cancel over the face of a receiver which extends over the layer depth. In effect the receiver will average the received signal over the area of its face(1):

$$v_{rn} = \int_0^d \frac{4}{\pi} \sum_{n=1}^{\infty} \left(\frac{1}{2n-1}\right) \sin \frac{(2n-1)\pi z}{d} \quad . \tag{2.39}$$

Evaluation of the above integral gives

$$v_{rn} = \frac{8d}{\pi} \sum_{n=1}^{\infty} \left(\frac{1}{2n-1}\right)^2 . \tag{2.40}$$

Therefore each mode contributes as $\left(\frac{1}{2n-1}\right)^2$ or 1, 1/9, 1/25, 1/49, for the first four excited modes.

A computer program was written to evaluate the effects of these higher modes on the solutions developed. Computer predictions considering (a) the fundamental mode alone and (b) the fundamental mode plus the next four non-zero higher modes, were plotted versus delayed-time. Comparison of these two predictions as presented graphically by the computer showed changes in the amplitude of less than 1 per cent and shifts in axis crossings of less than 0.01 local wavelengths. Since these effects are negligible compared to the experimental errors encountered in this research, it was sufficient to retain only the fundamental mode (n = 1).

Examination of Eq. 2.36 shows that it consists of two terms. The first (main) term is from the duct solution and the second (correction) term is from the layer effect. An estimate of the effect of the correction term can be made by combining the leading terms of the indicated

sums. Equation 2.36 can be rewritten as

$$\sqrt{\frac{r}{a}}\,\frac{\omega_n}{2}\left(\frac{t-T}{t+T}\right)^{-1/2}\xi_{rn} \doteq J_1(ARG) - \frac{3c}{4a\omega_n}\left(1-\frac{a}{r}\right)\left(\frac{t-T}{t+T}\right)^{1/2} J_2(ARG) \qquad (2.41)$$

Under the assumption $t' = t-T \ll T$, which limits consideration to the leading portion of the transient waveform, we have $t \approx T$, and Eq. 2.41 becomes

$$\sqrt{\frac{r}{a}}\,\frac{\omega_n}{2}\left(\frac{t'}{2T}\right)^{-1/2}\xi_{rn} \doteq J_1(\theta) - B(t)\,J_2(\theta) \qquad (2.42)$$

where $\theta = ARG = \omega_n\sqrt{t'2T}$

and $B(t) = \frac{3}{4}\frac{c}{a\omega_n}\left(1-\frac{a}{r}\right)\left(\frac{t'}{2T}\right)^{1/2}.$

Substitution of trigonometric approximations of the Bessel functions[13] in Eq. 2.42 gives

$$\sqrt{\frac{\pi\omega_n}{2}\frac{r}{a}}\;\omega_n T\,\xi_{rn} \doteq \cos\left(\theta-\frac{3\pi}{4}\right) - B(t)\cos\left(\theta-\frac{5\pi}{4}\right). \qquad (2.43)$$

By combining the cosine terms of Eq. 2.43, we find the expression for the fragment of radial particle displacement to be

$$\sqrt{\frac{\pi\omega_n}{2}\frac{r}{a}}\;\omega_n T \doteq \sqrt{1+B(t)^2}\;\cos\left(\theta-\frac{3\pi}{4}+\gamma\right) \qquad (2.44)$$

where $\gamma = \tan^{-1}B(t)$.

Equation 2.44 shows that the correction term in the layer solution introduces a phase angle γ that was not present in the duct solution. The zeroes of the right hand side of Eq. 2.44 give the times for which the particle displacement vanishes. It has been shown that the duct solution becomes the leading term of the layer solution; therefore, the zeroes of the first term of Eq. 2.43 give the nulls, or axis crossings, of the particle displacement in a duct. If these times are evaluated, the shift in time of associated axis crossings between the layer and the duct solutions can be predicted.

The zeroes of the layer solution, designated by τ_m, are obtained when

$$\cos\left(\theta - \frac{3\pi}{4} + \gamma\right) = 0, \tag{2.45}$$

or

$$\theta - \frac{3\pi}{4} + \gamma = \left(\frac{2m-1}{2}\right)\pi, \; m=1,2,3,\text{etc.} \tag{2.46}$$

The zeroes of the duct solution will be designated by ζ_{om}.
They are obtained when

$$\cos\left(\theta - \frac{3\pi}{4}\right) = 0, \tag{2.47}$$

or when

$$\left(\theta - \frac{3\pi}{4}\right) = \left(\frac{2m-1}{2}\right)\pi, \quad m = 1, 2, 3, \text{etc.} \tag{2.48}$$

Since we have $t' \ll T$, $c/a\omega_n < 1$, and $r \approx a$, so that

$$\tan\gamma = B(t) = \frac{3}{4}\frac{c}{a\omega_n}\left(1 - \frac{a}{r}\right)\sqrt{\frac{t'}{2T}} \ll 1, \tag{2.49}$$

a small-angle approximation can be applied with the result

$$\tan\gamma \doteq \gamma = \Gamma\,\zeta_m^{1/2} \tag{2.50}$$

where

$$\Gamma = \frac{3}{4}\frac{c}{a\omega_n}\left(1 - \frac{a}{r}\right)\frac{1}{\sqrt{2T}}.$$

Substituation of this expression for γ into Eq. 2.46 and evaluation of Θ in Eqs. 2.46 and 2.48 gives

$$\left(\omega_n\sqrt{2T} + \Gamma\right)\tau_m^{1/2} = \left(\frac{2m-1}{2} + \frac{3}{4}\right)\pi \tag{2.51}$$

and

$$\left(\omega_n\sqrt{2T}\right)\tau_{om}^{1/2} = \left(\frac{2m-1}{2} + \frac{3}{4}\right)\pi \, . \tag{2.52}$$

Manipulation of Eqs. 2.51 and 2.52 reveals that the ratio τ_m/τ_{om} can be expressed as

$$\frac{\tau_m}{\tau_{om}} = \frac{1}{1 + \frac{3}{4}\frac{a}{r}\left(c/a\omega_n\right)^2 + \frac{9}{64}\left(\frac{a}{r}\right)^2\left(c/a\omega_n\right)^4} \, . \tag{2.53}$$

Thus, $\frac{a}{r}\left(c/a\omega_n\right)^2$ is a convenient parameter to use in predicting the shift in axis crossings.

This result is approximate, since only the first terms of the sums in Eq. 2.36 were used to develop it. To evaluate the accuracy of this approximate result, computer programs were designed to evaluate the predicted waveforms of Eqs. 2.33 and 2.35 - 2.37. They were written so that the main terms and the correction terms of these equations could be evaluated separately. This permitted comparison of

the layer solutions and the duct solutions and showed the behavior of the correction term as a function of $c/a\omega_n$. These programs, one for the step input (Appendix A) and one for the gated sine-wave input (Appendix D) consider up to 11 terms of the sums involved. The programs give printed and graphical output of the main terms, the correction terms, and the complete expressions of the equations mentioned above. Figure 2.2 shows the velocity fragment predicted by the computer. Figures 2.3 - 2.5 show the complete expression, the main term, and the correction term of the displacement fragment for several values of $c/a\omega_n$.

Information about the envelope of the displacement fragment waveform can also be obtained from Eq. 2.44 which gives the amplitude as $\sqrt{1+B(t)^2}$. Under the assumption $t' << T$, $B(t)$ becomes

$$B(t) = \frac{3}{4}\frac{c}{a\omega_n}\left(\frac{r-a}{r}\right)\sqrt{\frac{t'}{2T}} \tag{2.54}$$

and

$$B(t)^2 = \frac{9}{32}\left(\frac{c}{a\omega_n}\right)^2\left(\frac{c}{r}\right)^2 T\, t' \tag{2.55}$$

Therefore, the amplitude of the initial portion of the waveform under consideration is

$$\sqrt{1 + \frac{9}{32}\left(\frac{c}{a\omega_n}\right)^2\left(\frac{c}{r}\right)^2 T t'} \; .$$

The approximate solutions for the propagation of simple transients in an isovelocity layer have been obtained, and computer programs to evaluate these solutions and predict the axis-crossings and amplitude-modulation in the layer have been written.

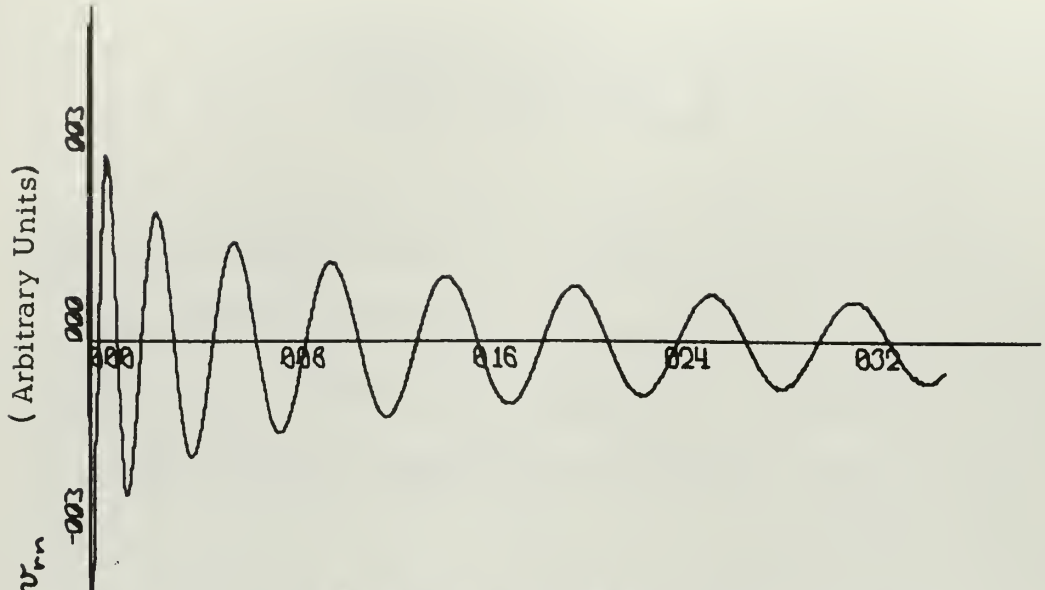

(a) Step input with $c/a\omega_n = 0.69$, $r = 61.5$ cm, $a = 2.54$ cm, and $d = 5.5$ cm.

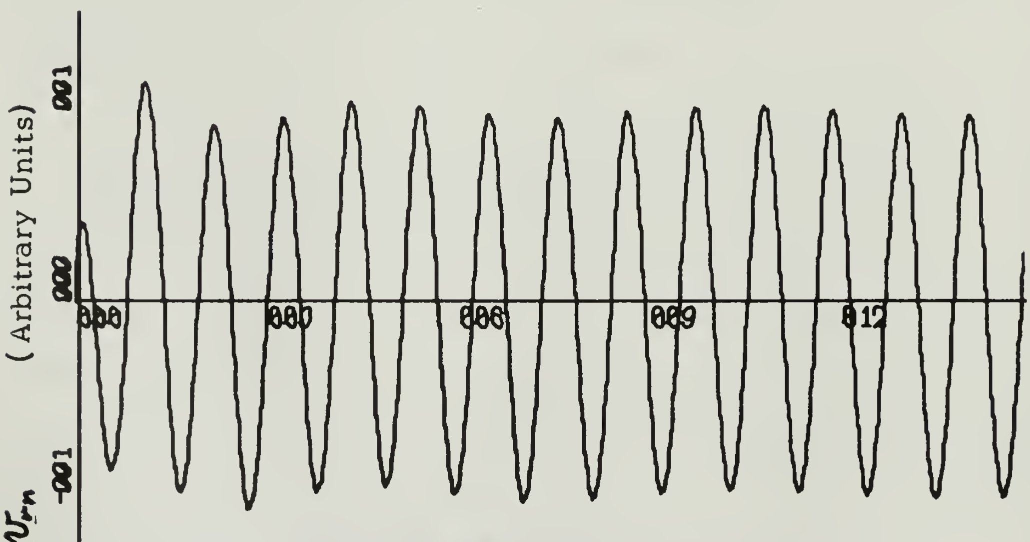

(b) Gated sine wave input with $c/a\omega_n = 1.00$ $r = 61.5$ cm, $a = 2.54$ cm, $d = 7.97$ cm, $\omega = 583$ kHz.

Fragment of radial particle velocity, v_{rn}, vs. delayed time, t'.

Figure 2.2

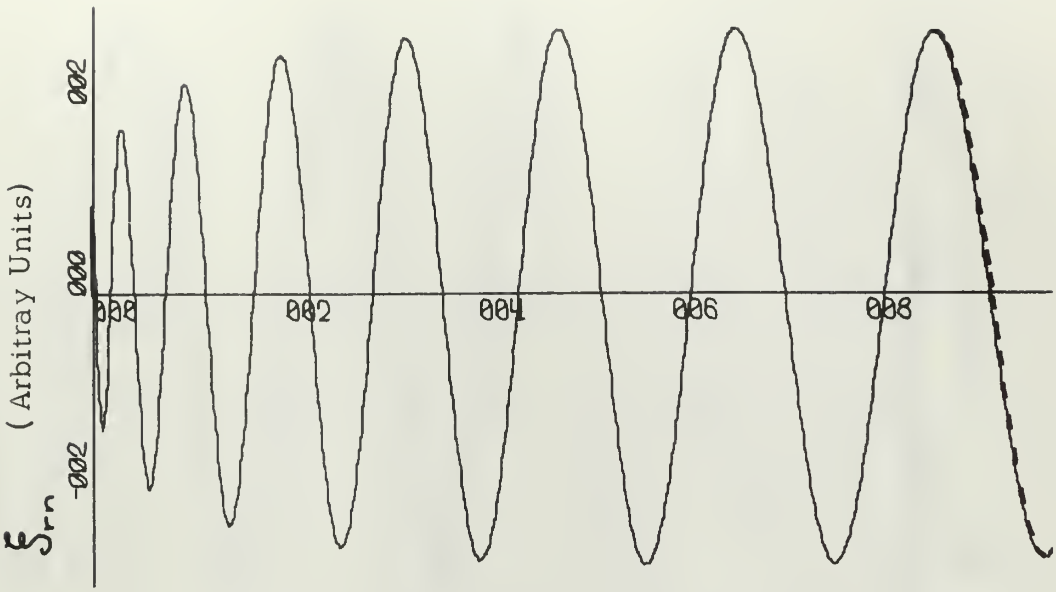

(a) Complete expression (layer solution) ————
Main term (duct solution) — — — — —

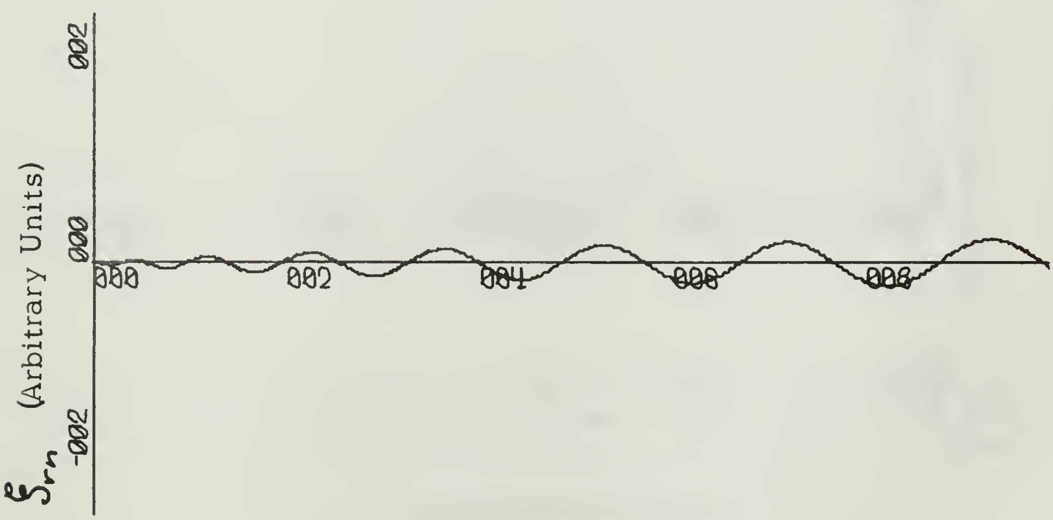

(b) Layer correction term

Fragment of the radial particle displacement, ξ_{rn}, vs. delayed time, t', as predicted by the computer program. $c/a\omega_n = 0.35$, $r = 61.5$ cm, $a = 2.54$ cm, $d = 2.80$ cm.

Figure 2.3

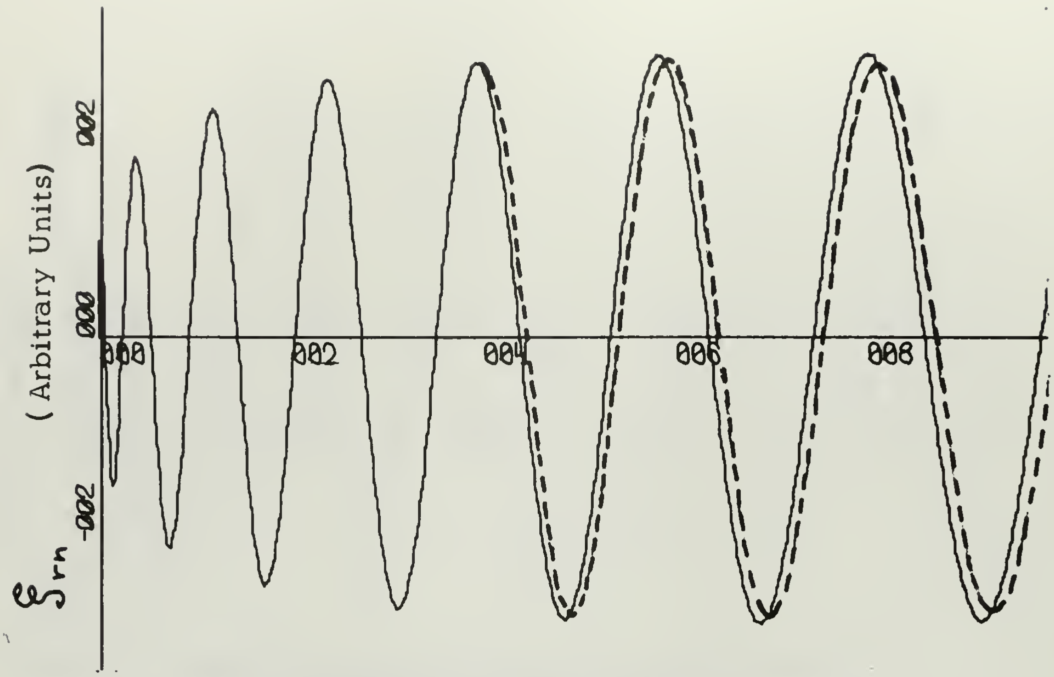

(a) Complete expression (layer solution) ————————
Main term (duct solution) – – – – – – – –

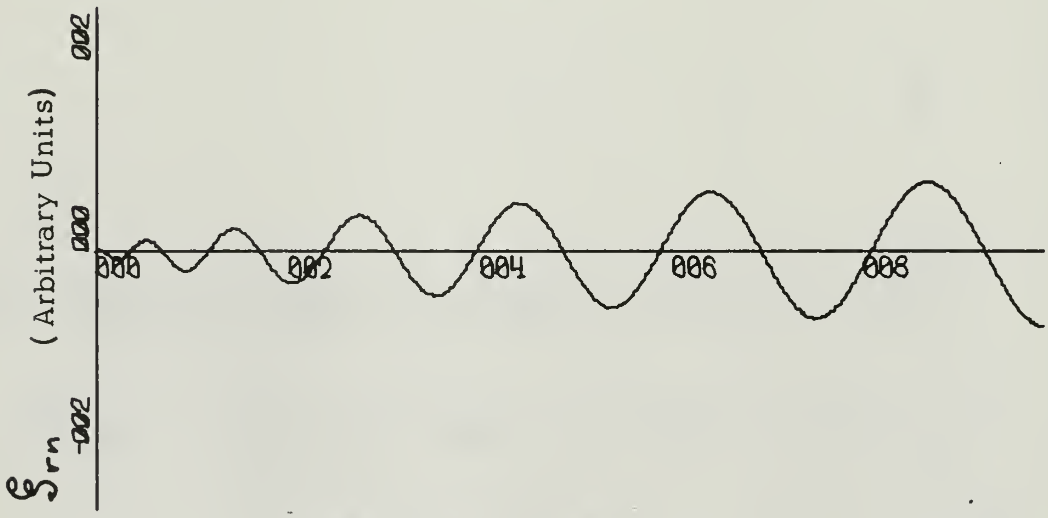

(b) Layer correction term

Fragment of the radial particle displacement, ξ_{rn}, vs. delayed time, t', as predicted by the computer program. $c/a\omega_n = 1.00$, $r = 61.5$ cm, $a = 2.54$ cm, $d = 7.97$ cm.

Figure 2.4

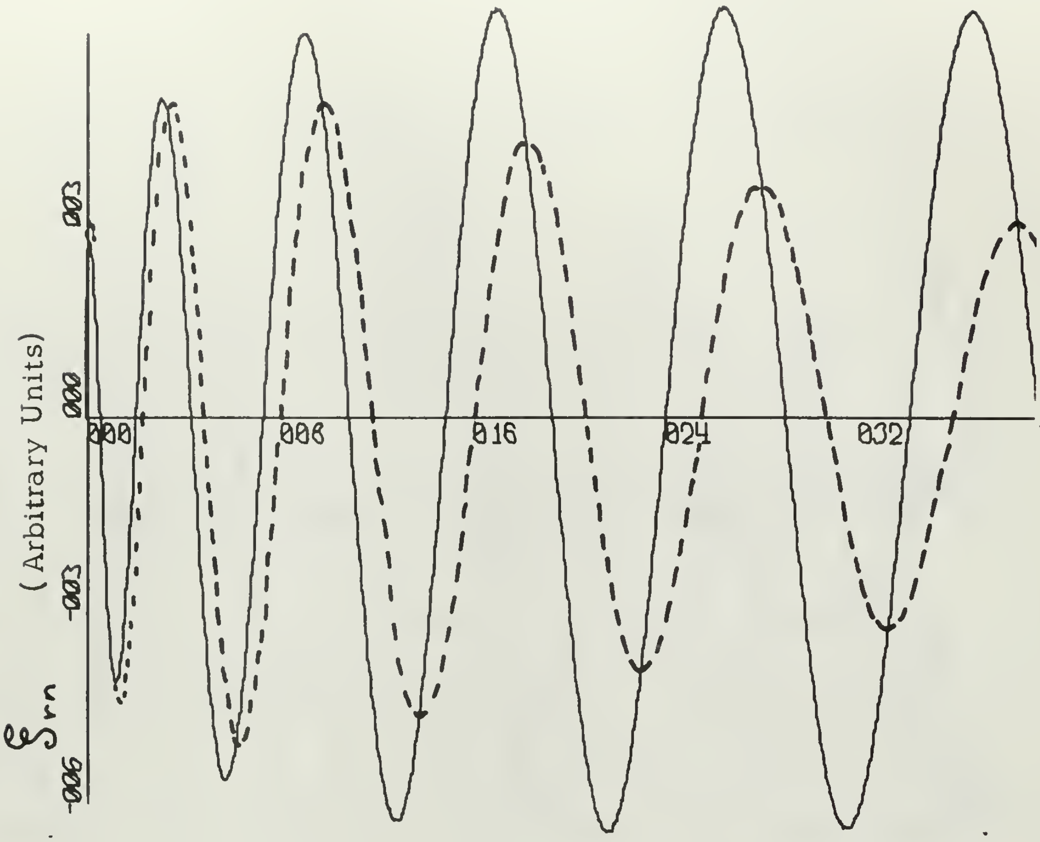

Complete expression (layer solution) ————

Main term (duct solution) - - - - - - -

Fragment of the radial particle displacement, ξ_{rn}, vs. delayed time, t', as predicted by the computer program. $c/a\omega_n = 3.00$, $r = 61.5$ cm, $a = 1.00$ cm, $d = 9.42$ cm.

Figure 2.5a

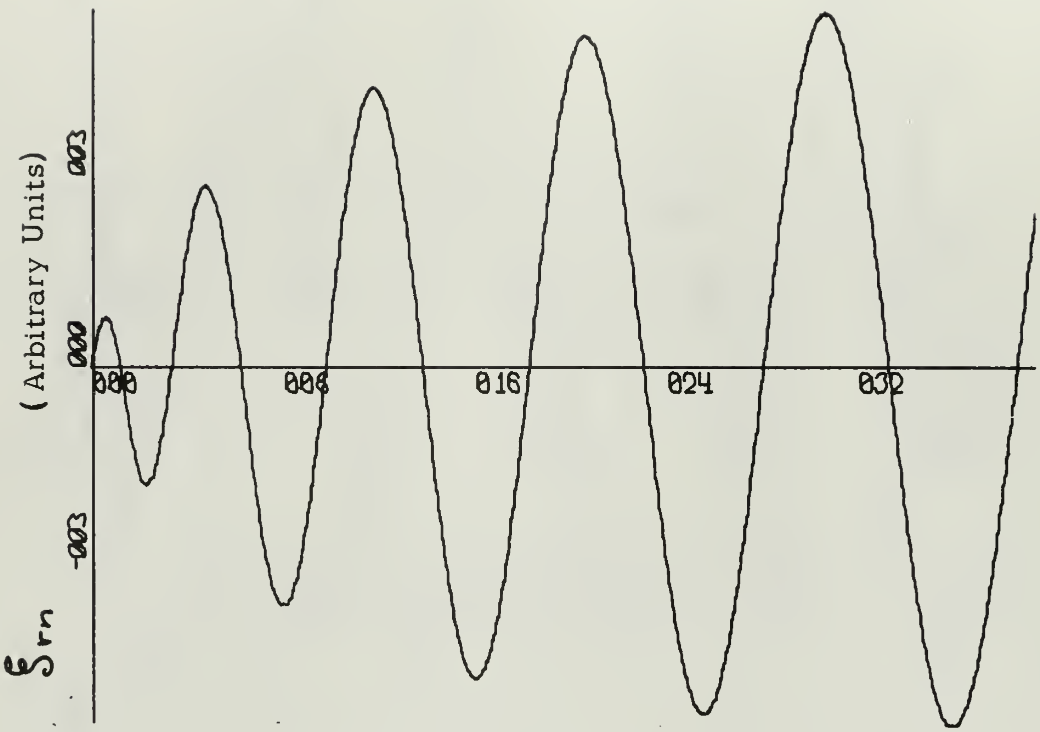

Layer correction term

Fragment of the radial particle displacement, ξ_{rn}, vs. delayed time, t', as predicted by the computer program. $c/a\omega_n = 3.00$, $r = 61.5$ cm, $a = 1.00$ cm, $d = 9.42$ cm.

Figure 2.5b

3. EXPERIMENTAL APPARATUS

The experimental apparatus used in this research consisted of a tank, several transmitters and receivers, and the associated electronics equipment. The laboratory setup is shown in Fig. 3.1.

Tank

The water layer was contained in a tank constructed of 3/4 inch marine plywood which was 30 cm high, 1 m wide, and 1.5 m long. The plywood was coated with Varathene to provide waterproofing, and lined with 1/4 inch polyethylene foam. This provided the desired pressure-release bottom boundary for the layer. The water-air interface provided the top pressure release surface. With the sides and ends of the tank also lined with polyethylene, the tank could be excited as a pressure-release cavity which served to accurately determine the depth of the layer. This technique is described in more detail in section 4.

Cylindrical sources could not be used because the tank was too small. Transmitters were therefore built in the shape of semi-cylinders and mounted on a rigid plate. A neoprene-coated steel plate, 3/8 inch thick, was made to fit in one end of the tank to act as the rigid boundary. This rigid surface served as an acoustical mirror, so that the reflected pressure appeared to be emitted from an image source (an identical semi-cylinder back-to-back with

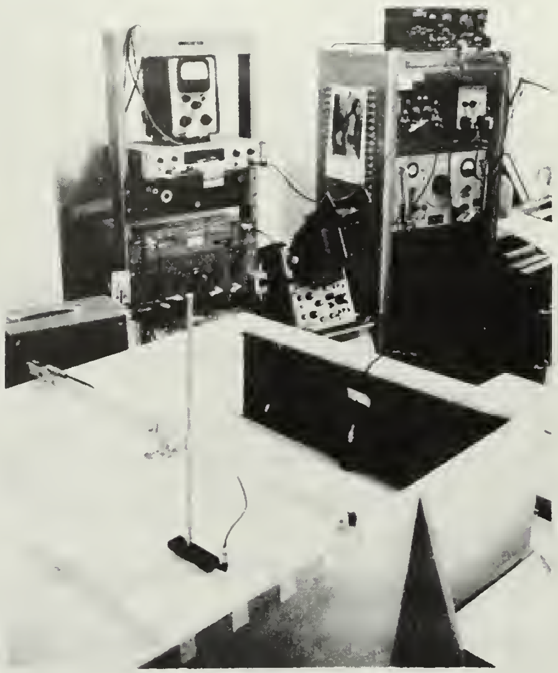

Tank with receiver, transmitter, and end plate in place. Electronics equipment in background.

Laboratory Setup

Figure 3.1

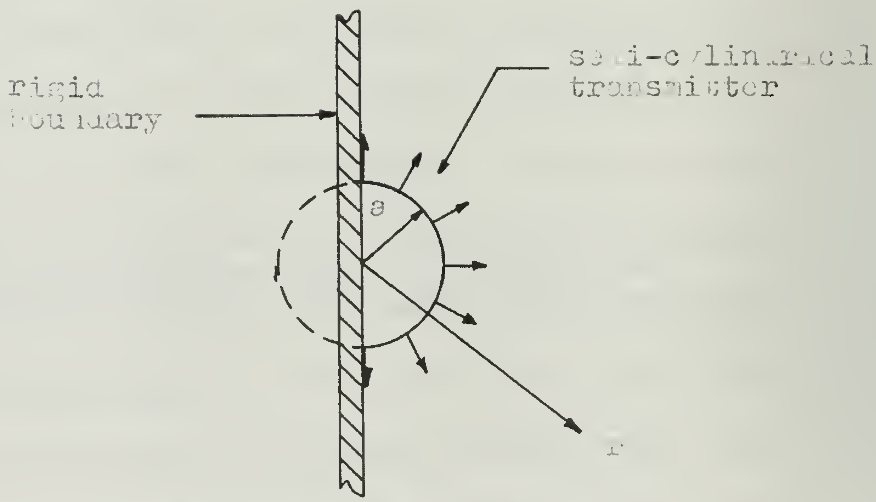

Geometry of Layer. (top view)

Figure 3.2

the real source). Under this condition cylindrical symmetry was approximated. Figure 3.2 illustrates the geometry of the layer.

Transducers

Mylar dielectric transducers were selected to be used in the layer for the following reasons:

(a) Their broad-band transmitting and receiving characteristics allowed the transmission and reception of the transient excitations without introducing significent frequency-sensitive modulation of the signals.

(b) They could be conveniently constructed to the required semi-cylindrical shapes and sizes.

(c) Previous work[16,17] has indicated that, when driven with a low-impedance voltage source, they generate an acoustic signal for which the normal particle velocity at the source is proportional to the input voltage.

Two transmitters were constructed to the required semi-cylindrical shape, using the techniques described in[17], one with radius 1.0 cm and one with radius 2.5 cm. Both transmitters were 12 cm high which corresponded to the maximum layer depth to be encountered. These dimensions were chosen in order to cover the desired range of values for $c/a\omega_n$.

A Mylar dielectric receiver, identical in nature to the transmitters, but with a plane, rectangular face measuring

3 cm x 14 cm, was used to measure the averaged (over depth) radical particle velocity and displacement in the layer. By proper adjustment of its electrical load, the receiver could be made sensitive to either particle velocity or displacement. When terminated by the 1 megohm impedance of the voltage amplifier, it was displacement sensitive; when shunted with an impedance of 100 ohms, it became sensitive to velocity. Transmitters and receivers are shown in Figure 3.3.

Two pressure-sensitive receivers were constructed, but neither proved to be satisfactory. A probe using a 1/8 inch barium titanate cylinder as the sensing element was built, but its low sensitivity resulted in an unacceptable signal to noise ratio. A 2.5 cm x 2.5 cm sensing element cut from a 0.5 cm Glennite disc was also constructed. However, the resonant frequency of the element was sufficiently close to the frequencies at the front of the received waveform so that ringing of the element caused severe distortion of the received signal. For this reason, and because it was felt that the velocity and displacement measurements would adequately describe the waveforms, pressure measurements were not taken.

Electronics Equipment

Figure 3.4 shows the block diagram of the equipment; Table 3.1 identifies the items in the figure. The oscillator

On the left, a 2.5 cm radius backplate and finished transmitter; center, partially completed and finished receivers; on the right, the 1.0 cm radius transmitter.

Transmitters and Receivers

Figure 3.5

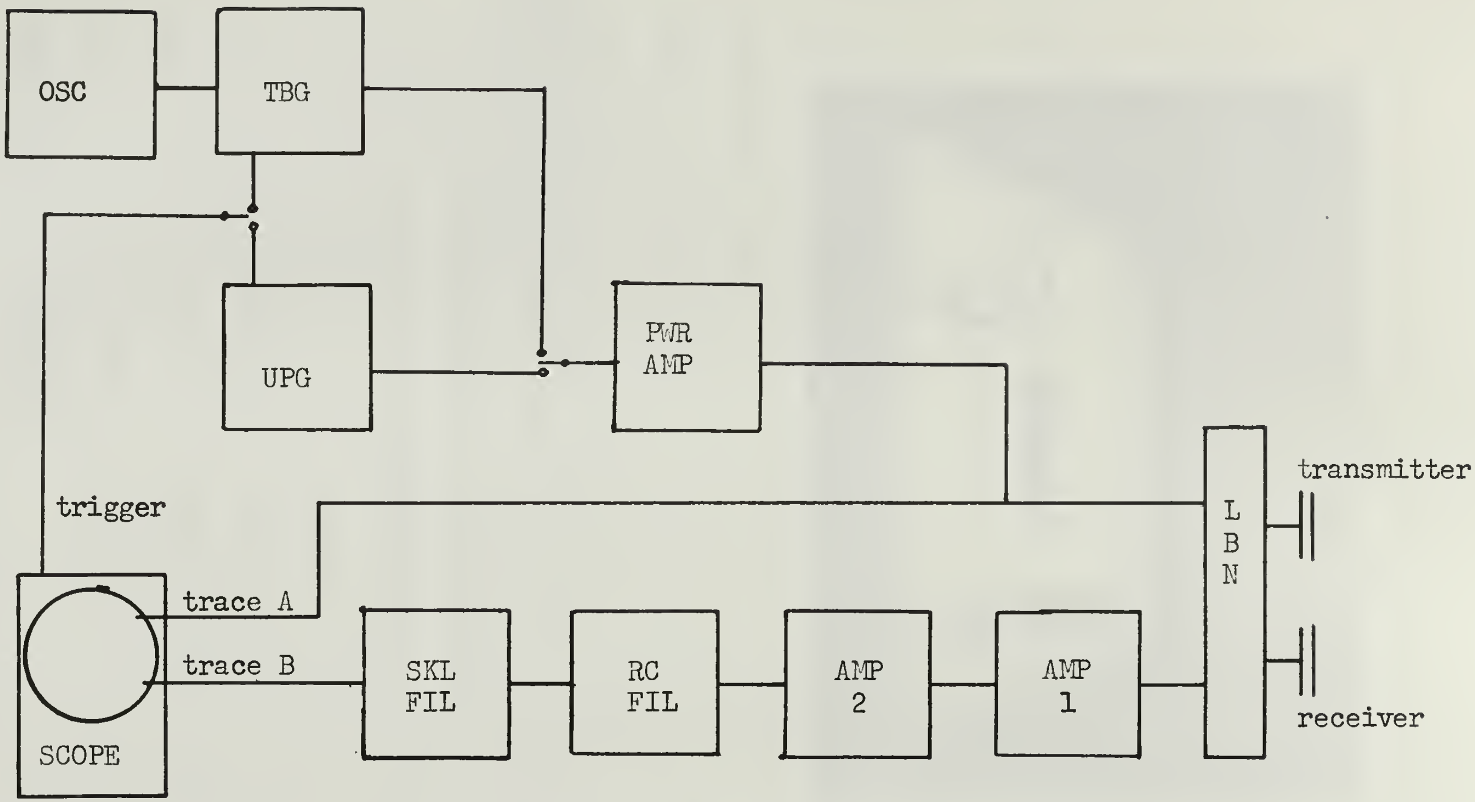

Block diagram of electronics equipment. Identified in table 3.1.

Figure 3.4

Table 3.1

Electronics Equipment

OSC	Audio oscillator, TS-382 D/U
TBG	Tone burst generator, General Radio type 1396-A
UPG	Unit pulse generator, General Radio type 1217-A
FREQ	Electronic counter, Hewlett Packard 5233-L
PWR AMP	Power amplifier, Hewlett Packard 467-A
AMP 1	Voltage amplifier, Teletronix type 1121
AMP 2	Wide band chain amplifier, SKL model 202-D
RC FIL	Homemade variable low-pass RC filter with 400 kH_z roll-over.
SKL FIL	Electronic band pass filter SKL model 302
SCOPE	Dual beam oscilloscope, Fairchild model 766-H
LBN	Load and bias network (made for earlier work) shown in Fig. 3.5

and tone burst generator were used as the initial signal source for the gated sine-wave input. For the step input, the unit pulse generator was used.

The received signal was sent from the receiver through the load and bias network, amplifiers, and filters to trace "B" of the dual beam oscilloscope. The input signal taken from the output of the power amplifier was displayed on trace "A". Measurements of the received waveform axis crossings and amplitudes were made directly from the oscilloscope display, or photographed for later analysis. Triggering of the scope was provided by gating signals from either the tone burst generator or the unit pulse generator. The load and bias network shown in Figure 3.5 served to supply the 300 volt bias needed by the Mylar transducers without allowing this voltage to appear elsewhere in the circuit, and to provide the proper electrical load for the receiver so that either particle displacement or velocity could be observed. The 22 ohm resistor in the transmitter circuit was needed to suppress parasitic oscillations caused by the transient electrical excitation of the capacitance of the transmitter and the residual inductance of the power amplifier.

The rise time of the system was experimentally determined to be about 0.5 μ sec.

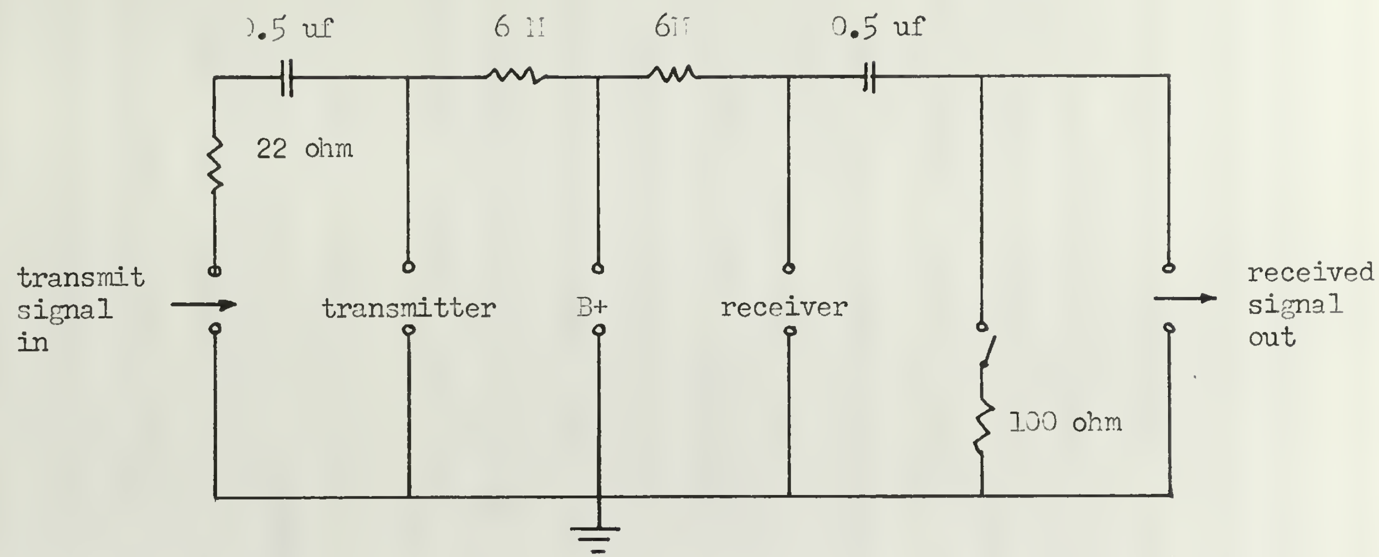

Load and bias network

Figure 3.5

4. EXPERIMENTAL INVESTIGATION

The purpose of the experimental investigation was to (a) observe and analyze the received radial particle-velocity and displacement waveforms in an isovelocity layer; (b) compare these waveforms with theoretical waveforms produced as output of computer programs based on the theoretical developments; and (c) vary the parameter $c/a\omega_n$ over a range of values to see if the solutions broke down when the basic restriction $c/a\omega_n < 1$ was violated. The greater part of the experimental investigation was made using the step-function input; the gated-sine wave input was used only infrequently. Experiments were conducted using the procedure described in the following paragraphs. Five basic variables characterized each experiment; the input function (gated sine-wave or step-function), the range r, the transmitter radius a, the layer depth d, and the speed of sound c.

Experimental Procedure

Since $c/a\omega_n$ was a fundamental parameter of the solutions, the input function and the value of $c/a\omega_n$ to be used were first chosen for each run. The 2.5 cm transmitter was used for values of $c/a\omega_n$ from 0.35 to 1.00; the 1.0 cm transmitter was used for values ranging from 1.00 to 3.00. The temperature of the water was measured to determine the speed of sound c in the layer[18].

With a, c, and the desired value of $c/a\omega_n$ determined the necessary value of ω_n could be calculated. The tank was then filled to a convenient depth and excited as a pressure-release cavity of known length and width. The depth of water was adjusted until the maximum resonance peak of the fundamental mode was observed at the desired ω_n. From ω_n and the known length and width of the tank the effective depth was calculated for the computer program which was written with depth rather than ω_n as an input. The end plate and transmitter were placed in the tank, an input signal was fed to the transmitter, and the receiver was placed at the range of 61.5 cm (used in all experiments) by measuring the time-of-flight of the signal from transmitter to receiver.

The received waveforms were photographed from the oscilloscope display. For the step input, several photographs were taken of each waveform. An expanded time scale was used for photographs of the leading portion of waveform where the high frequencies were contained; a more compressed time scale was used for suceeding photographs. For a typical experiment, three photographs of each waveform were made utilizing, for example, 5 μsec/cm, 10 μsec/cm, and 50 μsec/cm time scales. For the step input experiments, both received particle displacement and velocity were photographed in most cases. The photo-

graphs were then read using dividers and a scale to determine the values of delayed time τ_m at which axis crossings occured. The amplitudes of the peaks in the waveform were measured in a similiar fashion. Sample photographs are shown in Fig. 4.1. Data read from all photographs are contained in Appendix B.

For each experimental run, a corresponding computer run was made using the same values for r, a, c, and d (and hence $c/a\omega_n$) as inputs to the computer program. As has been shown in Section 2, a solution for particle displacement or velocity in the layer can be expressed as the sum of the corresponding duct solution and a "layer correction." The computer programs could therefore be written so that their output for each run contained a series of graphs of the duct solution, layer solution, and "layer correction" waveforms. The program for the step input produced a series of graphs for both particle displacement and velocity waveforms. The program for the gated-sine input graphed the velocity series only. Comparison of graphs within a series provided convenient visual evidence of the relative importance of the "layer correction" with respect to the duct solutions as a function of the parameter $c/a\omega_n$. A portion of the step input program was used to find the axis crossings of the theoretical displacement waveforms for the duct and layer solutions.

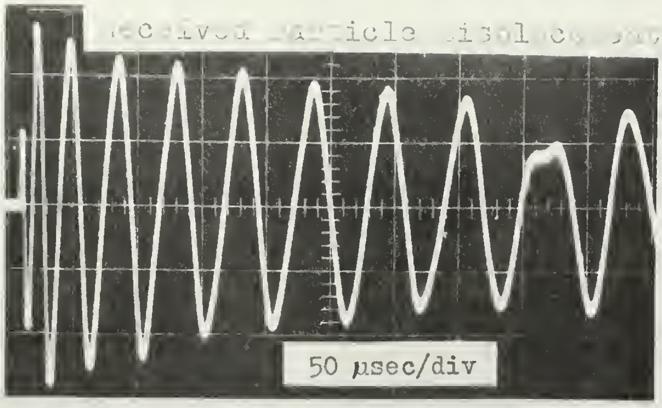

Step Input
in Velocity

$c/a\omega_n$ = 0.5[illegible]

r = 51.[illegible] cm

a = [illegible].5 cm

d = 5.[illegible] cm

temp = 20° C.

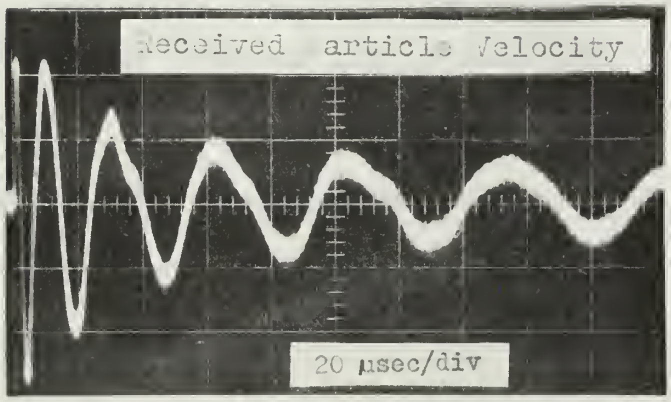

Step Input
in Velocity

$c/a\omega_n$ = 0.69

r = 51.[illegible] cm

a = [illegible].5 cm

d = 5.5 cm

temp = [illegible]° C.

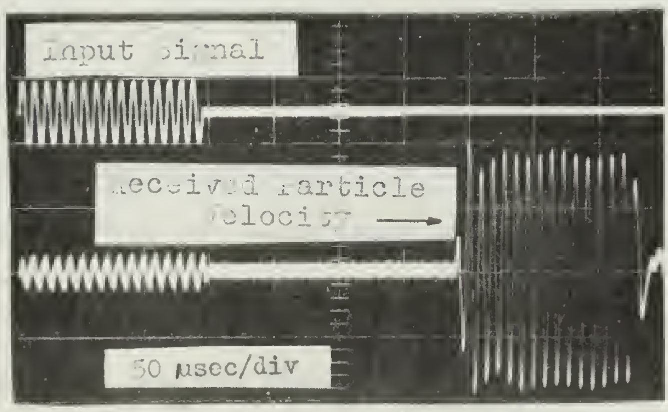

Gated Sine Wave
Input in Velocity

ω = 5[illegible].[illegible] kHz

$c/a\omega_n$ = 1.[illegible]

r = 51.[illegible] cm

a = [illegible] cm

d = [illegible] cm

temp = [illegible]° C.

[illegible]

[illegible]

Another portion of the program evaluated the magnitude and delayed time of the amplitude peaks in the layer-solution displacement waveform. In this manner the theoretical values of τ_{om} and τ_m, and the magnitudes of times of the peak amplitudes could then be compared with the observed values of τ_m and amplitude peaks found in the experiment with the corresponding value of $c/a\,\omega_n$.

Analysis of Data

Analysis of the response of the layer to a step-function input proved to be more involved than was originally estimated. For this reason, and because of the limited time available for this investigation, data from the runs performed with a gated sine-wave input were not analyzed. The following analysis pertains to the step-function input data only.

Recall that the simple theory in Section 2 based on the trigometric approximations for the Bessel functions suggested that if values of τ_m are plotted versus τ_{om}, a straight line should result. This relationship would offer advantages in data reduction because a family of axis crossings could be summarized by the slope of a straight line. For this reason, graphs which plotted the observed and computed values of τ_m versus the computed values of τ_{om} were made for each run. Figures 4.2 - 4.4 are representative examples of these graphs. The solid line of

unit slope represents the computed values of τ_{om}. The circles are the computed values of τ_m, and the crosses are the observed values of τ_m. It is clear that each set of points can be joined by a straight line which quantitatively describes by its slope the predicted and observed shift in time of the layer solution axis crossings as compared with those of the duct.

A graph was then made which plotted the predicted and observed values of $\frac{\tau_m}{\tau_{om}}$ versus $c/a\omega_n$ (Fig. 4.5). The simple theory would suggest plotting $\frac{\tau_m}{\tau_{om}}$ versus $a/r\,(c/a\omega_n)^2$, however, r was fixed for all experiments and only two values of a were used. Furthermore it is the validity of the layer solutions for various values of $c/a\omega_n$ which is the topic of investigation here, rather than the validity of Eq. 2.53.

Analysis of the amplitude peak data was also made for step input solutions. The experimental amplitude peaks read from each waveform photograph were first normalized to the value of the highest peak in the waveform. The predicted peaks were normalized in the course of the computer program. The ratio of these normalized quantities was then plotted as a function of the delayed time of the predicted amplitude peaks for each run. Exact agreement in the shape of the transient waveform between experiment and theory would result in a line of zero slope. Figure 4.6 shows plots for three values of $c/a\omega_n$.

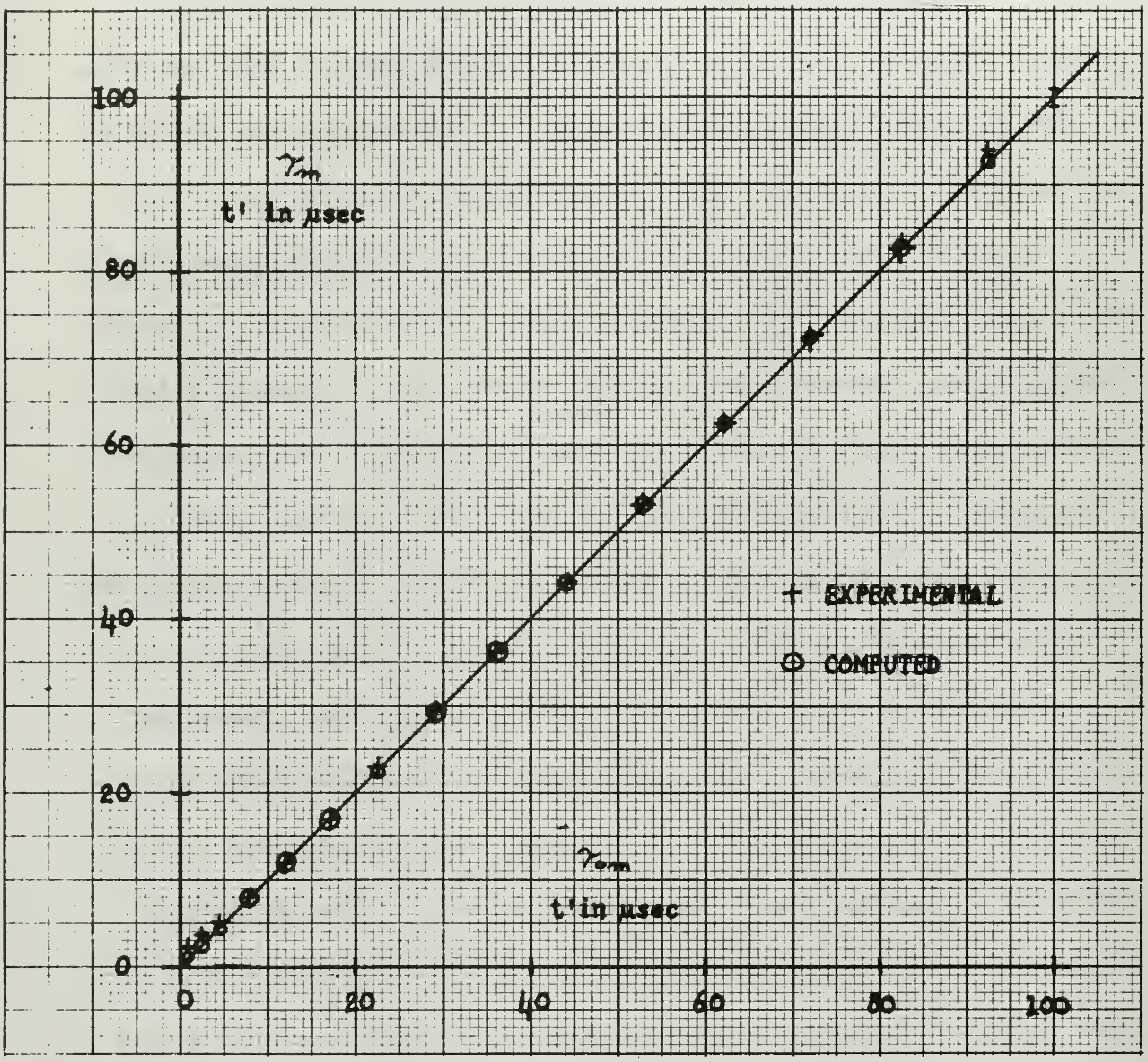

$c/a\,\omega_n = 0.35$
$r = 61.5$ cm

$a = 2.5$ cm
$d = 2.80$ cm
temp = 20° C.

Experimental and Computed τ_m vs. τ_{om} Particle Displacement Waveform Generated by a Step Input in Velocity.

Figure 4.2

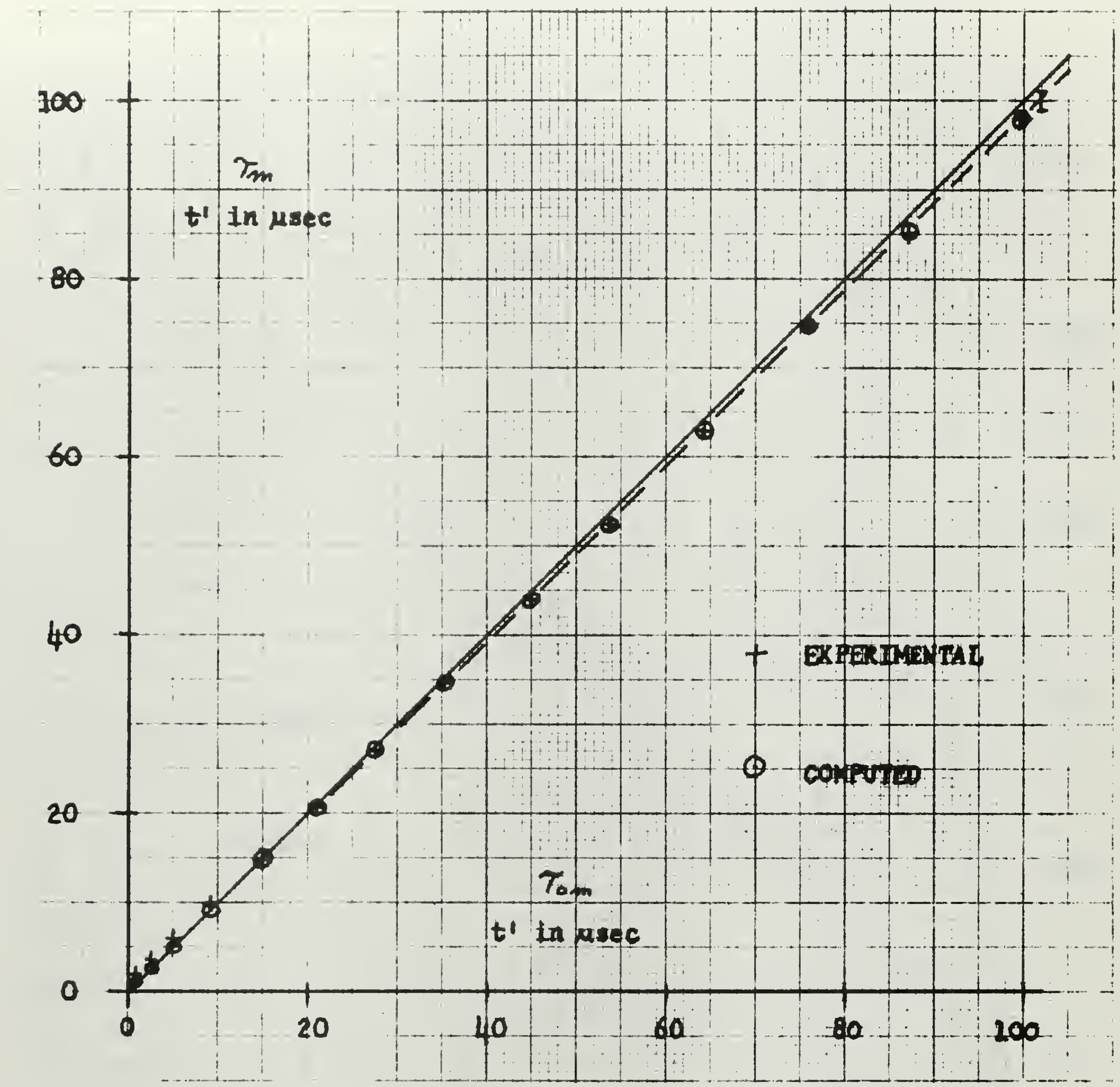

$c/a\omega_n = 1.00$
$r = 61.5$ cm

$a = 1.0$ cm
$d = 3.14$ cm
temp = 20° C.

Experimental and Computed τ_m vs. τ_{om} Particle Displacement Waveform Generated by a Step Input in Velocity.

Figure 4.3

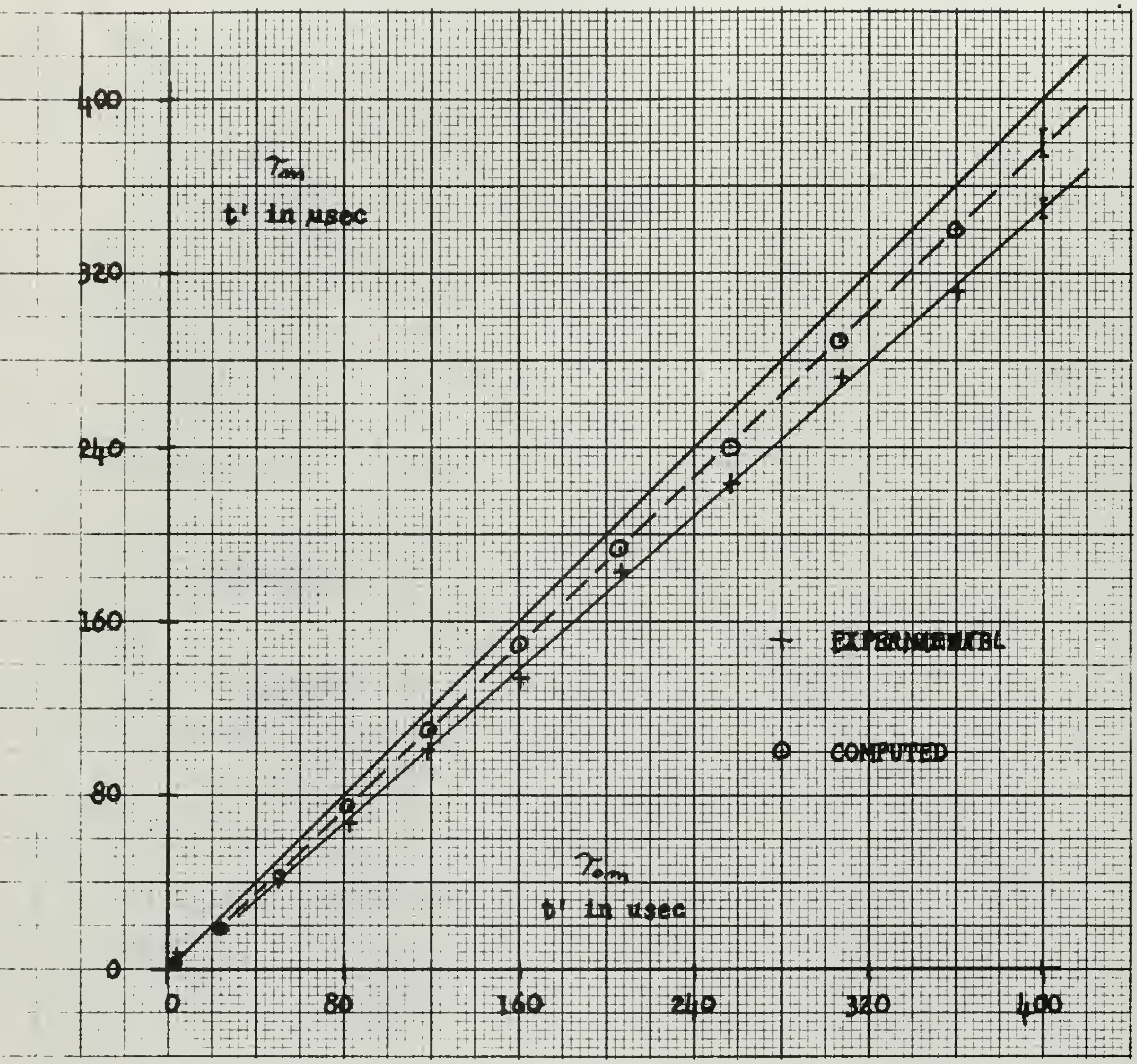

$c/a\,\omega_n = 3.00$ $\quad$ $a = 1.0$ cm
$r = 61.5$ cm $\quad$ $d = 9.42$ cm
temp = 20° C.

Experimental and Computed τ_m vs. τ_{om} Particle Displacement Waveform Generated by a Step Input in Velocity.

Figure 4.4

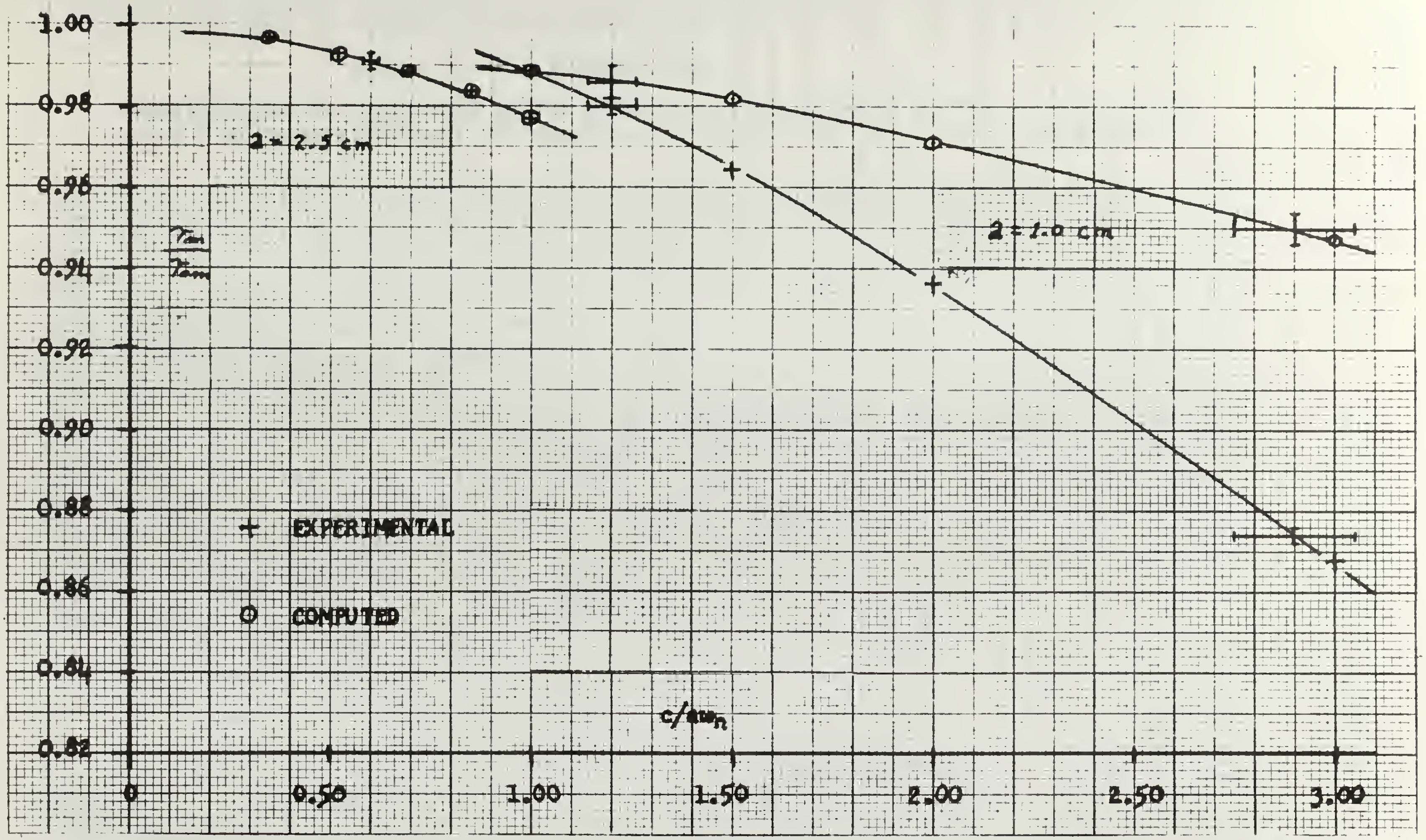

Experimental and Computed $\frac{\tau_m}{\tau_{om}}$ vs. $c/a\omega_n$ for Particle Displacement Waveform Generated by a Step Input in Velocity.

Figure 4.5

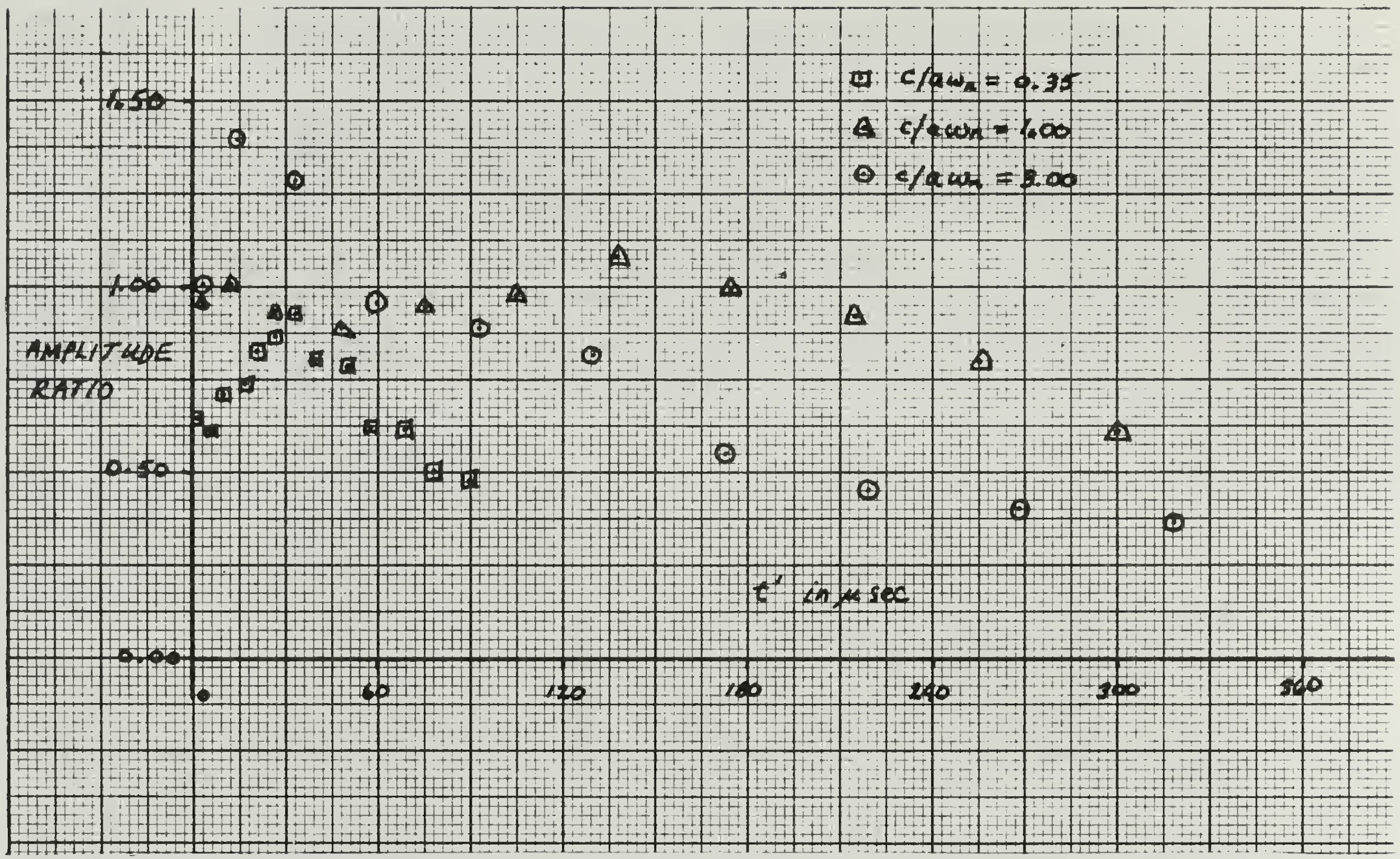

Ratio of Experimental to Observed Normalized Particle Displacement Amplitudes vs. Delayed Time Generated by a Step Input in Velocity

Figure 4.6

Error Analysis

An analysis of the assumption that the semi-cylindrical source and steel backplate combination could be used in lieu of a cylindrical source was necessary. The complex impedance of the plate was evaluated from relations in[19] for the range of frequencies contained in the received waveforms. The impedance mis-match was sufficiently large to justify assuming that the plate was rigid. The directivity of each transmitter when mounted on the steel plate was investigated in order to compare the resulting radiation pattern with the uniform radiation assumed in the theoretical deveopment. Directivity patterns are shown in Figs. 4.7 and 4.8. In order to determine the effect of the deviation of the actual patterns from the theoretical patterns, each transmitter was clamped with foam rubber so that only a 90 degree arc in the center of the transmitter was radiating sound. Except for small change s in amplitude, no differences were observed in the received waveforms as compared to those received for radiation over the full 180 degrees of the transmitter. It was therefore assumed that radiation from the transmitters could be assumed uniform and that the transmitter-plate combination could be used to approximate a cylindrical source.

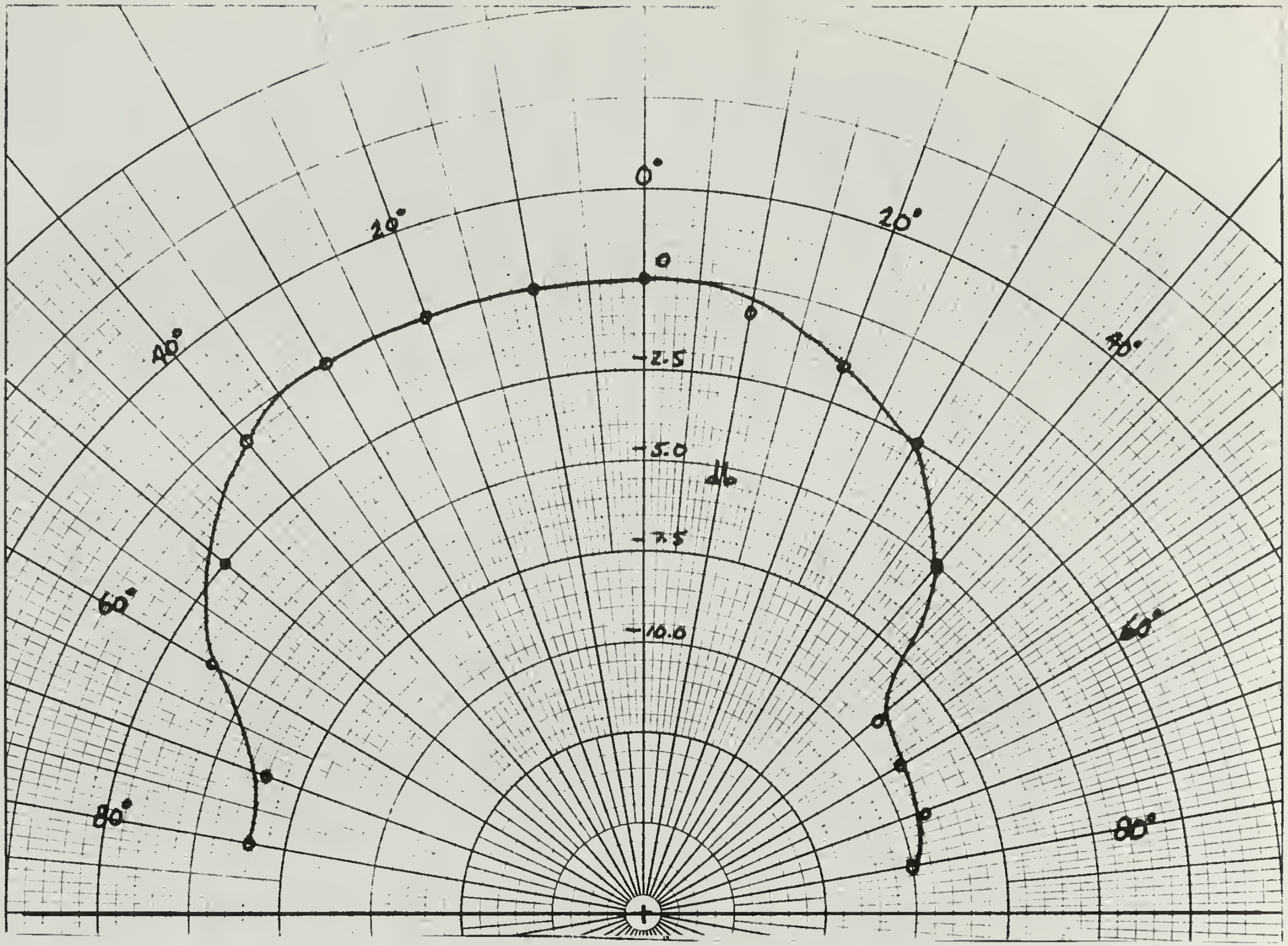

r = 27.0 cm
d = 5.50 cm

Step Input
in Velocity

Directivity Pattern for 1.0 cm radius Transmitter.

Figure 4.7

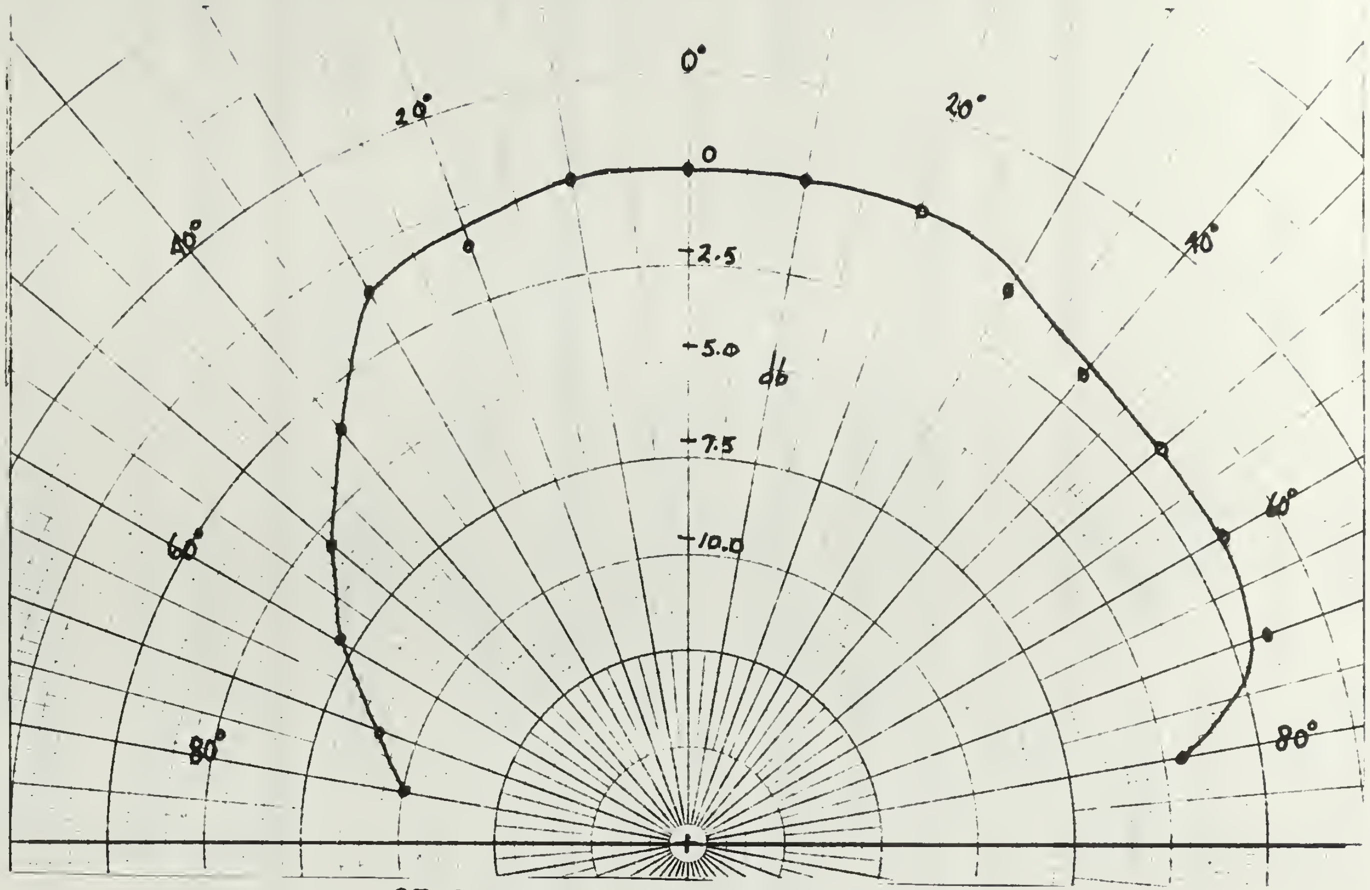

r = 27.0 cm
d = 5.50 cm

Step Input
in Velocity

Directivity Pattern for 2.5 cm radius Transmitter.

Figure 4.8

The rise time of the experimental system was determined to be about 0.5 μsec. Therefore, instead of being a perfect step-function input, the velocity at the source was initially described by

$$V_a(t) = 1 - e^{-\alpha t}$$

where $\alpha = 2 \times 10^6 \text{ sec}^{-1}$ is the reciprocal of the rise time.

The group velocity of the waveform is given by

$$c_g = \frac{r}{T+t'} = c\sqrt{1-(\omega_n/\omega)^2}. \qquad (4.1)$$

Under the condition $\omega \gg \omega_n$, and with $\frac{r}{c} \approx T$, Eq. 4.1 can be written as

$$\frac{T}{T+t'} \approx 1 - \frac{1}{2}(\omega_n/\omega)^2$$

By rearranging Eq. 4.1, the value of delayed time at which a frequency ω will appear in the received waveform can be expressed as

$$t' \approx \frac{T}{2}\left(\frac{\omega_n}{\omega}\right)^2.$$

It would be expected that the amplitudes of frequencies greater than α contained in the initial portion of the received waveforms would be depleted up to a time given by

$$t' \approx \frac{T}{2}\left(\frac{\omega_n}{\alpha}\right)^2, \qquad (4.2)$$

and that amplitude distortion of the waveforms would be significant up to this time. However, substitution of the observed α and the largest value of ω_n experimentally encountered into Eq. 4.2, shows that distortion would be

significant at the most for only 1.5 μsec. Therefore the rise time of the system should have no great effect on the received waveforms.

It was necessary to investigate the characteristics of the transmitters to see if the velocity of the face remained proportional to the step input voltage over the interval of time that the received waveforms were studied. For times much greater than the rise time, the mass of the diaphram can be ignored provided its velocity remains reasonably constant over the time interval of interest. The resulting equivalent circuit of the transmitter with a source resistance added(17) is shown in Fig. 4.9. Writing loop equations for the equivalent circuit gives

$$e - iR_s - \frac{1}{C_0}\int i\,dt + \frac{1}{C_0}\int \beta V_a\,dt = 0$$

$$\frac{1}{\beta^2 C_s}\int \beta V_a\,dt + \beta V_a\left(\frac{A\rho c}{\beta^2}\right) - \frac{1}{C_0}\int i\,dt = 0$$

which enables us to write the Laplace transform of the diaphram velocity as

$$\bar{V}_a = \frac{s\bar{e}}{\left(\frac{C_0 R_s A\rho c}{\beta}\right)s^2 + \left(\frac{A\rho c}{\beta} + \frac{C_0 R_s}{\beta C_s}\right)s + \left(\frac{1}{\beta C_s} - \frac{\beta}{C_0}\right)} \qquad (4.3)$$

β is determined from the electro-mechanical relationships of the transmitter and is defined as(17)

$$\beta = \frac{C_0 E_0}{x_0} .$$

Nominal equivalent circuit values for the 1 cm radius transmitter with a 20 volt step input applied are shown in Fig. 4.9. Substituting these values into Eq. 4.3 and taking the inverse transform yields

$$V_a = 3.4 \times 10^{-4} e^{-360t}.$$

Since the mass of the transmitter diaphram is ignored in this approximation, the particle velocity is a maximum immediately after the application of the step input and then decays exponentially. Substituting t=360 μsec (the longest interval of delayed time over which received waveforms were observed) into Eq. 4.3 shows that the velocity has decayed to 88 percent of its maximum value at the end of this time. The tailing off of the amplitude peaks of the received waveforms, as shown in Fig. 4.6, is consistent with the decay in velocity of the transmitter diaphram.

Uncertainties in a, c, r, ω_n, and τ_m were the possible sources of error in this investigation. The effective radius of each transmitter was measured to the nearest 1/2 mm, which could have introduced an uncertainty of $\pm$ 2 percent in the value of a for the 2.5 cm radius transmitter, and $\pm$ 5 percent in the value of a for the 1.0 cm radius transmitter. Measurement of the temperature of water to the nearest degree restricted the (systematic) error in c to within $\pm$ 0.5 percent. The method of determining T, the time-of-flight of the signal from transmitter to

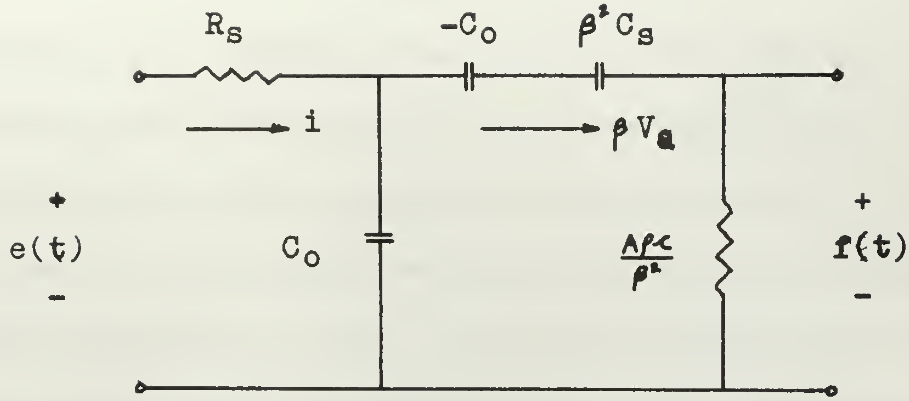

R_s = 22 ohm

C_o = 1000 pf

$A = 3.8 \times 10^{-3}\ m^2$

$\rho c = 1.5 \times 10^6$ kg/sec-m^2

$C_s = 10^{-6}$ m/N

E_o = 300 volts

$x_o = 3 \times 10^{-5}$ m

$\beta = 10^{-2}$ N/volt

e(t) = 20 volt step input

Equivalent circuit of transmitter
Figure 4.9

receiver, gave a possible systematic error of $\pm$ 0.5 percent, which in turn resulted in an estimated error in r of $\pm$ 0.5 percent.

Two sources of error were possible in the determination of ω_n by excitation of the tank as a pressure-release cavity. Observed irregularities of $\pm$ 1/4 mm in the bottom surface of the tank could introduce an error in the local effective depth of the layer. Since experiments were always conducted in the same portion of the tank, a systematic error in ω_n would result. This error could range from $\pm$ 0.3 percent (for the 9.42 cm depth) to $\pm$ 1 percent (for the 2.80 cm depth). The random error possible in determining the frequency of the resonance peaks of the standing wave spectrum proved to be insignificant relative to the possible systematic error.

The experimental values of τ_m could be influenced by systematic errors on the order of $\pm$ 1 percent caused by nonlinearity and miscalibration of the oscilloscope time-base. As mentioned previously in this section, axis crossing times were read from a series of photographs with different time scales. This method was used so that the initial portion of the received signal would always be at the left-hand edge of the picture and the axis crossings of interest would generally occur in the right half plane of the display. This procedure resulted in a random error of $\pm$ 0.5 percent

on all time scales since the display could be read to within 1/4 scale division out of 50 divisions.

The errors in the computed values of τ_m were influenced predominately by the error in ω_n, since ω_n appears in the argument of the Bessel functions ($\omega_n\sqrt{t^2-T^2}$) from which the τ_m's are computed. The values of τ_m were determined when the argument equaled any one of a set of constants C_m which resulted in a zero value for the amplitude of the particle-displacement solution. Thus the argument can be written as

$$\omega_n\sqrt{t_m^2-T^2} = \omega_n\sqrt{(t_m-T)(t_m+T)} = \omega_n\sqrt{\tau_m(\tau_m+2T)} = C_m$$

and if we have $\tau_m \ll T$, then

$$\omega_n\sqrt{2T}\,\tau_m^{1/2} \approx C_m$$

and

$$\tau_m \approx C_m^2/\omega_n^2\,2T \,.$$

Therefore the $\pm$ 1 percent error in ω_n could lead to $\pm$ 2 percent error in the computed values of τ_m .

The errors in the slopes of the curves fitted to the experimental τ_m's in Figs. 4.2 - 4.4 were determined mainly by the systematic errors in these values of τ_m because the random errors were minimized by fitting a straight line through the points. Therefore the error in each slope was estimated to be $\pm$ 1 percent. There was a systematic error of $\pm$ 2 percent in the computed values of τ_m ; hence the error in the slope of the computed τ_m versus τ_{om} lines was $\pm$ 2 percent.

The errors in c, a, and ω_n being independent can be combined by the root-mean-square law to yield the error in c/a ω_n. The percent error in c/a ω_n varied according to the values of a and ω_n involved. Table 4.1 shows the result of this combination for representative values of c/a ω_n. Error flags on Figs. 4.2 - 4.5 indicate the relative magnitudes of errors in the experimental and computed values of τ_m and slopes, and the relative magnitude of error in c/a ω_n.

Table 4.1

Tabulated Errors for Quantities Displayed on Figures 4.2-4.5

	Percent Error					
$c/a\omega_n$	c	a	ω_n	$c/a\omega_n$	Exp. slope	Comp. slope
0.35	± 0.5	± 2.0	± 1.0	± 2.3	± 1.0	± 2.0
1.00	0.5	2.0	0.3	2.1	1.0	2.0
1.00	0.5	5.0	0.8	5.1	1.0	2.0
3.00	0.5	5.0	0.3	5.0	1.0	2.0

5. RESULTS AND CONCLUSIONS

The investigation has shown that for $c/a\,\omega_n \leq 1$, the predicted and experimentally observed shift in axis crossings agreed to within $\pm$ 2 percent. Where the restriction $c/a\,\omega_n < 1$ was violated, the theory failed to predict the observed shift in axis crossings. As $c/a\,\omega_n$ was increased the failure of the theory became more pronounced.

The correlation between the predicted and observed amplitudes was less favorable. The divergence between the predicted and observed amplitudes in the initial portion of the received signal was unexplained. The decrease in the observed amplitudes in the latter portion of each received signal is not inconsistent with the roll-off of the step-function input in velocity.

Therefore, with the exception of amplitudes, we can say that the theoretical solutions correctly described the propagation of simple transients in an isovelocity layer with perfectly-reflecting boundaries as long as the parameter $c/a\,\omega_n$ was ≤ 1; and that, although the theory failed for values of $c/a\,\omega_n > 1$, it did correctly predict the trend that the observed waveforms followed.

BIBLIOGRAPHY

1. D.V. Anderson and C. Barnes, "The Dispersion of a Pulse Propagated through a Cylindrical Tube," J. Acoust. Soc. Am. 25, 525-528 (1953).

2. J.M. Proud, P.T. Tamarakin, and E.T. Kornhauser, "Propagation of Sound Pulses in a Dispersive Medium," J. Acoust. Soc. Am. 28, 80-85 (1956).

3. K. Walther, "Pulse Compression in an Acoustic Waveguide," J. Acoust. Soc. Am. 33, 681-686 (1961).

4. A.B. Coppens, "Exact Solutions for the Propagation of Two Simple Acoustic Transients in Waveguides with Perfectly-Reflecting Walls," J. Acoust. Soc. Am. 40, 331-341 (1966).

5. W.C. Knudsen, "Propagation of a Pressure Transient in a Two Layer, Liquid Model," J. Acoust. Soc. Am. 29, 918-924 (1957).

6. L.M. Brekhovskikh, Waves in Layered Media, trans. D. Lieberman. (Academic Press, New York, 1960), Chap. 5.

7. J.R. Wait, "Propagation of Pulses in Dispersive Media," J. Res. Natl. Bur. Std. (U.S.). 69D, 1287-1401 (1965).

8. J. W. Miles, "On Radiation and Scattering from Small Cylinders," J. Acoust. Soc. Am. 25, 1087-1089 (1953).

9. R.G. Barakat, "Propagation of Acoustic Pulses from a Circular Cylinder," J. Acoust. Soc. Am. 33, 1759-1764 (1961).

10. C.M. Knop, "Pulsed Electromagnetic Wave Propagation in Dispersive Media," IEEE Trans. On Antennas and Propagation. AP12, 494-496 (1964).

11. C.T. Case and R.E. Haskell, "On 'Pulsed Electromagnetic Wave Propagation in Dispersive Media'," IEEE Trans. on Antennas and Propagation. AP14, 401 (1966)

12. A.B. Coppens, "Approximate Relationship between Propagation of Transients in Waveguides of Constant Cross-Section and in Isovelocity Layers of Cylindrical Symmetry," Unpublished Letter. (1966).

13. U.S. Department of Commerce, Handbook of Mathematical Functions, ed. M. Abramowitz and I. Stegum. (U.S. Government Printing Office, Washington, D.C., June 1964), Chap. 9.

14. E.N. Dekanosidze, Tables of Lommel Functions of Two Variables, trans. D.G. Fry. (Permagon Press, Inc. New York, 1966).

15. G.N. Watson, Treatise on the Theory of Bessel Functions, (The McMillan Company, New York, 1945), 2nd Ed.

16. G.R. Schodder and F. Wiekhorst, "Electrostatic Transducers with Solid Dielectrics for Waterborne Sound," Acustica. 7, 38-45 (1957).

17. G.L. Palatini, Electroacoustic Properties of Mylar Dielectric Underwater Sound Transducers, Thesis, Naval Postgraduate School, Monterey, California(1966).

18. M. Greenspan and C.E. Tschiegg, "Tables of the Speed of Sound in Water," J. Acoust. Soc. Am. 31, 75-76 (1959).

19. L.E. Kinsler and A.R. Fry, Fundamentals of Acoustics (John Wiley & Sons, Inc., New York, 1962), end Ed., Chap. 6.

APPENDIX A

A-1: Summary of the Propagation of Transients in Waveguides.

Results for the propagation of simple transients (step-function and gated sine-wave input) in ducts which have appeared in the literature [4,10] and which will be of value in this research are presented below along with some additional Laplace transform pairs that are needed.

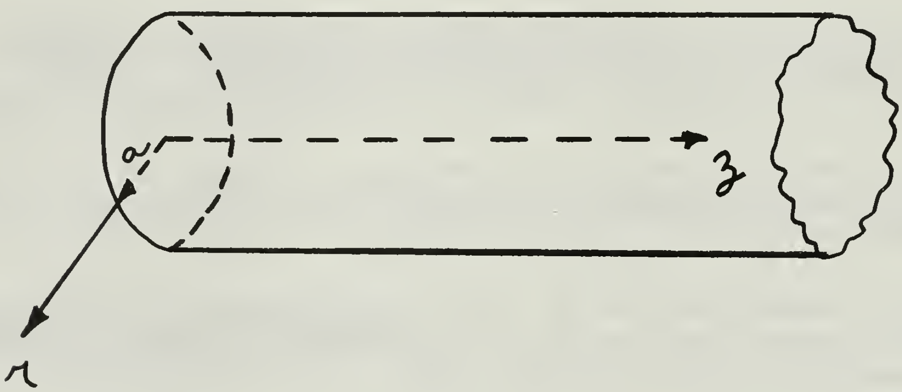

Figure A.1

Assume a waveguide of uniform cross-section, infinite length, and perfectly-reflecting boundaries, which is filled with a lossless fluid and excited by a velocity souce at z = 0. See Fig. A.1 The wave equation for the acoustic velocity potential Φ can be written in cylindrical coordinates as

$$\left(\frac{\partial^2}{\partial r^2} + \frac{1}{r}\frac{\partial}{\partial r} + \frac{\partial^2}{\partial z^2} - \frac{1}{c^2}\frac{\partial^2}{\partial t^2}\right)\Phi(r,z,t) = 0 \qquad \text{(A.1)}$$

where r is the radial direction, z is the longitudinal direction, and radially symmetric processes have been assumed.

The separation of variables

$$\Phi(r,z,t) = \sum_n \Phi_n(r,z,t) = \sum_n R_n(r)\,\phi_n(z,t) \qquad \text{(A.2)}$$

leads to the solution $R_n = J_o(\omega_n r/c)$ where J_o represents the zeroeth order Bessel function of the first kind, and the partial differential equation

$$\left[\frac{\partial^2}{\partial z^2} - \left(\frac{\omega_n}{c}\right)^2 - \frac{1}{c^2}\frac{\partial^2}{\partial t^2}\right]\phi_n(z,t) = 0 \qquad \text{(A.3)}$$

which describes the propagation in the z direction. The value of the separation constant ω_n depends on the nature of the boundary at r = a (the wall of the duct) and the cross-sectional area of the tube. Because the transverse properties of the duct affect only ω_n and not the form of the solution of Eq. A.3, all functions of r have been suppressed. They can be reintroduced with no difficulty when desired.

The Laplace transform of Eq. A.3 with quiescent initial conditions is

$$\frac{\partial^2}{\partial z^2}\bar{\phi}_n = \frac{s^2+\omega_n^2}{c^2}\bar{\phi}_n \qquad \text{(A.4)}$$

where the bar over the function indicates the Laplace transform of that function, and ϕ_n is a fragment of the velocity potential containing z and t. Solving Eq. A.4 with the boundary condition $\bar{\phi}_o = \bar{\phi}_n(0,t)$ gives

$$\bar{\phi}_n = \bar{\phi}_o \exp\left[-T\sqrt{s^2+\omega_n^2}\right] \tag{A.5}$$

where T = z/c is the time of flight of the signal from the source to the receiver.

The relation $u_{zn} = R_n \frac{\partial \phi_n}{\partial z}$ is used to obtain the Laplace transform of the fragment of the longitudinal particle velocity:

$$\bar{v}_{zn} \equiv \bar{u}_{zn}/R_n(r) = \frac{-\bar{\phi}_o\sqrt{s^2+\omega_n^2}}{c} \exp\left[-T\sqrt{s^2+\omega_n^2}\right]. \tag{A.6}$$

Application of the boundary condition on velocity at the source $v_n(0,t) = V_o(t)$ casts Eq. A.6 into the following form:

$$\bar{v}_{zn} = \bar{V}_o \exp\left[-T\sqrt{s^2+\omega_n^2}\right] \tag{A.7}$$

The relation

$$\bar{\phi}_o = \frac{-c\bar{V}_o}{\sqrt{s^2+\omega_n^2}} \tag{A.8}$$

is evident from examination of Eqs. A.6 and A.7. If this value of $\bar{\phi}_o$ is substituted into Eq. A.5, the Laplace transform of ϕ_n in terms of the velocity input becomes

$$\bar{\phi}_n = \frac{-c\bar{V}_o \exp\left[-T\sqrt{s^2+\omega_n^2}\right]}{\sqrt{s^2+\omega_n^2}} \tag{A.9}$$

The fragment of the longitudinal acoustic pressure is obtained from the velocity potential by means of the expression $p_{zn} \equiv p_n/R_n(r) = -\rho \frac{\partial \phi_n}{\partial t}$. This corresponds to $\bar{p}_{zn} = -\rho s\bar{\phi}_n$ in the Laplace transform domain. We therefore have the result

$$\bar{p}_{zn} = \frac{\rho c s \bar{V}_o}{\sqrt{s^2+\omega_n^2}} \exp\left[-T\sqrt{s^2+\omega_n^2}\right] \tag{A.10}$$

The fragment of longitudinal particle displacement may be obtained either by integrating the fragment of longitudinal particle velocity in the time domain or by multiplying by 1/s in the Laplace transform domain. With the latter alternative, the particle displacement fragment $\bar{\xi}_{zn}$ can be written as

$$\bar{\xi}_{zn} = \frac{\bar{V}_o}{s} \exp\left[-T\sqrt{s^2+\omega_n^2}\right] \tag{A.11}$$

Equations A.7 and A.9 - A.11 are the Laplace transforms of the acoustic variables of interest. The inverse transforms for a step-function input ($\overline{V}_o = 1/s$) and a gated sine-wave input ($\overline{V}_o = \frac{\omega}{s^2+\omega^2}$) are as follows:

For a step-function input

$$\phi_n = -\frac{c}{\omega_n}\, 2 \sum_{m=1}^{\infty} \left(\frac{t-T}{t+T}\right)^{\frac{2m-1}{2}} J_{2m-1}(ARG) \tag{A.12}$$

$$v_{zn} = J_0(ARG) + 2 \sum_{m=1}^{\infty} \left(\frac{t-T}{t+T}\right)^{m} J_{2m}(ARG) \tag{A.13}$$

$$p_{zn} = \rho c J_0(ARG) \tag{A.14}$$

$$\xi_{zn} = \frac{2}{\omega_n} \sum_{m=1}^{\infty} (2m-1) \left(\frac{t-T}{t+T}\right)^{\frac{2m-1}{2}} J_{2m-1}(ARG) \tag{A.15}$$

Where $ARG = \omega_n \sqrt{t^2 - T^2}$

For a gated sine-wave input:

$$\phi_n = \frac{c_p}{\omega}\left[U_0(w_+, ARG) - U_0(w_-, ARG)\right] \tag{A.16}$$

$$v_{zn} = U_1(w_+, ARG) + U_1(w_-, ARG) \tag{A.17}$$

$$\mathscr{P}_{3n} = e^{c_p}\left[U_1(w_+, ARG) - U_1(w_-, ARG)\right] \qquad (A.18)$$

$$\xi_{3n} = -\frac{1}{\omega}\left[U_0(w_+, ARG) - U_0(w_-, ARG) - 2\sum_{m=1}^{\infty}\left(\frac{t-T}{t+T}\right)^{m-1} J_{2m-2}(ARG)\right. \qquad (A.19)$$

Where $ARG = \omega_n \sqrt{t^2 - T^2}$

$$w_{\pm} = \omega(t-T)(1 \pm c_g/c)$$

The U's represent Lommel functions of two variables

$$U_\nu(w_\pm, ARG) = \sum_{m=0}^{\infty}(-1)^m\left(\frac{w_\pm}{ARG}\right)^{\nu+2m} J_{\nu+2m}(ARG)$$

A-2: Development of Additional Laplace Transform Pairs for Step Input in Velocity in an Isovelocity Layer.

The transform pairs developed in this section are those needed for the layer solution in addition to those summarized in section A-1. $\overline{F}$ denotes the transform under consideration; f(t) is the inverse transform of $\overline{F}$. All f(t)'s are defined as zero for $t \leq T$.

1.

$$\overline{F} = \frac{s\overline{V}_0 \exp\left[-T\sqrt{s^2+\omega_n^2}\right]}{s^2+\omega^2} \qquad (A.20)$$

With $\overline{V}_o = 1/s$, Eq. A.20 becomes

$$\overline{F} = \frac{\exp\left[-T\sqrt{s^2+\omega_n^2}\right]}{s^2+\omega^2} \tag{A.21}$$

Equation A.21 is of the same form as Eq. A.7 with $\overline{V}_o = \frac{\omega}{s^2+\omega^2}$ and $\omega = \omega_n$. Therefore the inverse transform of Eq. A.7 may be used with $\omega = \omega_n$. The inverse transform of Eq. A.7 is

$$U_1(w_+, ARG) + U_1(w_-, ARG) \tag{A.22}$$

where ARG = $\omega_n\sqrt{t^2-T^2}$

and $\quad w_\pm = \omega(t-T)(1 \pm c_g/c)$

The quantity c_g/c can be written as $\sqrt{1-(\omega_n/\omega)^2}$. With $\omega = \omega_n$, we have $w_+ = w_- = \omega_n(t-T)$. This in turn means that both terms of Eq. A.22 are equal. Using the relation[14],

$$2U_\nu\left[\omega_n(t-T), ARG\right] = 2\sum_{m=0}^{\infty}(-1)^m\left[\frac{\omega_n(t-T)}{ARG}\right]^{\nu+2m} J_{\nu+2m}(ARG) \tag{A.23}$$

the desired inversion is obtained. With $\nu = 1$ and ARG = $\omega_n\sqrt{t^2-T^2}$, Eq. A.21 may be rewritten as

$$f(t) = 2U_1(w, ARG) = 2\sum_{m=1}^{\infty}(-1)^{m-1}\left(\frac{t-T}{t+T}\right)^{\frac{2m-1}{2}} J_{2m-1}(ARG) \tag{A.24}$$

2.

$$\bar{F} = \frac{\bar{V}_0}{S} \frac{\exp\left[-T\sqrt{s^2+\omega_n^2}\right]}{\sqrt{s^2+\omega_n^2}} \tag{A.25}$$

With $\bar{V}_o = 1/s$, Eq. A.25 becomes

$$\bar{F} = \frac{\exp\left[-T\sqrt{s^2+\omega_n^2}\right]}{s^2\sqrt{s^2+\omega_n^2}} \, . \tag{A.26}$$

The identity

$$\frac{1}{x} = 2\sum_{\nu=0}^{\infty} \left[\frac{1}{\sqrt{1+x^2}+x}\right]^{2\nu+1} \tag{A.27}$$

is used to generate the desired inverse transform. Squaring Eq. A.27 gives

$$\left(\frac{1}{x}\right)^2 = 4\sum_{\nu=0}^{\infty} (\nu+1)\left[\frac{1}{\sqrt{1+x^2}+x}\right]^{2(\nu+1)} . \tag{A.28}$$

Letting $x = \omega n/s$ in Eq. A.28 and rearranging yields

$$\left(\frac{\omega_n}{s}\right)^2 = 4\sum_{\nu=0}^{\infty} (\nu+1)\left[\frac{\omega_n}{\sqrt{s^2+\omega_n^2}+s}\right]^{2(\nu+1)} . \tag{A.29}$$

Solving Eq. A.29 for 1/s and substituting the value obtained into Eq. A.26 results in

$$\bar{F} = \frac{1}{\omega_n^2}\left\{4\sum_{\nu=0}^{\infty}(\nu+1)\left[\frac{\omega_n}{\sqrt{s^2+\omega_n^2}+s}\right]^{2(\nu+1)} \frac{\exp\left[-T\sqrt{s^2+\omega_n^2}\right]}{\sqrt{s^2+\omega_n^2}}\right. \tag{A.30}$$

The inverse transform of Eq. A.30 is available[8]. Therefore with $\nu + 1 = m$,

$$f(t) = \frac{4}{\omega_n^2} \sum_{m=1}^{\infty} m \left(\frac{t-T}{t+T} \right)^m J_{2m}(ARG) \tag{A.31}$$

A-3: <u>Inverse Laplace Transforms for a Gated Sine-Wave Input in Velocity in an Isovelocity Layer</u>.

The following acoustic quantities could not be completely solved. Although the expressions listed are incomplete solutions, it is worthy of note that the leading terms are the corresponding terms of the duct solutions in Section A-1. In the equations listed $\mathcal{L}^{-1}\{\ \}$ denotes the inverse Laplace transform of the quantity in brackets.

$$\sqrt{\frac{r}{a}}\,\phi_n = \frac{c\rho}{\omega}\left[U_0(n\omega_+, ARG) - U_0(n\omega_-, ARG)\right] + \frac{3c^2\omega}{8a}\left(1+\frac{a}{3r}\right)\mathcal{L}^{-1}\left\{\frac{\exp\left[-T\sqrt{s^2+\omega_n^2}\right]}{(s^2+\omega^2)(s^2+\omega_n^2)}\right\} \tag{A.32}$$

$$\sqrt{\frac{r}{a}}\,p_{pm} = \rho c \rho\left[U_1(n\omega_+, ARG) - U_1(n\omega_-, ARG)\right] + \frac{3\rho c^2\omega}{8a}\left(1+\frac{a}{3r}\right)\mathcal{L}^{-1}\left\{\frac{s\exp\left[-T\sqrt{s^2+\omega_n^2}\right]}{(s^2+\omega^2)(s^2+\omega_n^2)}\right\} \tag{A.33}$$

$$\sqrt{\frac{F}{a}}\,\xi_{rn} = -\frac{1}{\omega}\left[U_0(w_+, ARG) + U_0(w_-, ARG) + 2\sum_{m=0}^{\infty}\left(\frac{t-T}{t+T}\right)^m J_{2m}(ARG)\right] \quad (A.34)$$

$$+ \frac{3c\omega}{8a}\left(1-\frac{a}{r}\right)\mathcal{L}^{-1}\left\{\frac{\exp\left[-T\sqrt{s^2+\omega_n^2}\right]}{s(s^2+\omega^2)\sqrt{s^2+\omega_n^2}}\right\}$$

where ARG = $\omega_n\sqrt{t^2-T^2}$

$$w_\pm = \omega(t-T)(1 \pm c_g/c)$$

$U_\nu(w_\pm, ARG)$ = Lommel Function of two variables[14,15].

$$U_\nu(w_\pm, ARG) = \sum_{m=0}^{\infty}(-1)^m\left(\frac{w_\pm}{ARG}\right)^{\nu+2m} J_{\nu+2m}(ARG)$$

APPENDIX B
EXPERIMENTAL DATA

DISPLACEMENT AXIS CROSSINGS TPRI IN USEC	DISPLACEMENT AMPLITUDES (NORMALIZED)	VELOCITY AXIS CROSSINGS TPRI IN USEC

STEP INPUT RUN S3
C/AWN=0.35 R=61.5CM A=2.54CM D=2.80CM TMP=20DEGC

0.0	0.175	0.95
1.10	-0.379	2.35
2.85	0.442	4.35
5.50	-0.592	7.65
9.00	0.660	11.3
13.3	-0.718	16.5
18.5	0.864	21.7
24.3	-0.922	28.2
30.8	1.000	34.3
38.0	-0.898	42.4
45.9	0.893	50.3
54.2	-0.718	59.2
63.8	0.718	68.2
73.5	-0.592	79.5
84.0	0.563	91.0
96.0		

STEP INPUT RUN S12
C/AWN=0.52 R=61.5CM A=2.54CM D=4.15CM TMP=20DEGC

0.0	0.198	NOT RECORDED
2.50	-0.396	
5.10	0.636	
10.7	-0.833	
17.7	1.000	
26.1	-0.972	
36.6	0.905	
48.4	-0.860	
61.3	0.838	
76.0	-0.838	
91.7	0.721	
108.5	-0.694	
126.0	0.622	
145.0	-0.613	
164.0	0.532	
184.5	-0.477	

DISPLACEMENT AXIS CROSSINGS TPRI IN USEC	DISPLACEMENT AMPLITUDES (NORMALIZED)	VELOCITY AXIS CROSSINGS TPRI IN USEC

STEP INPUT RUN S6

C/AWN=0.69 R=61.5CM A=1.00CM D=5.50CM TMP=20DEGC

0.0	0.414	2.20
3.50	-0.687	6.70
9.60	0.990	14.4
18.4	-1.000	23.2
29.8	0.919	38.6
45.8	-0.909	52.5
64.0	0.828	73.5
85.0	-0.854	93.0
106.0	0.798	119.0
131.0	-0.727	140.0
168.0	0.768	169.0
183.0	-0.687	193.0
212.0	0.687	
240.0	-0.657	
268.0	0.667	
298.0	-0.581	
329.0	0.616	
360.0		

STEP INPUT RUN S13

C/AWN=0.85 R=61.5CM A=2.54CM D=6.78CM TMP=21DEGC

0.0	0.357	NOT RECORDED
4.20	-0.697	
13.6	0.871	
26.3	-0.874	
44.5	0.994	
65.9	-0.931	
90.2	0.777	
118.0	-0.834	
147.5	1.000	
179.5	-0.943	
212.5	0.783	

DISPLACEMENT AXIS CROSSINGS TPRI IN USEC	DISPLACEMENT AMPLITUDES (NORMALIZED)	VELOCITY AXIS CROSSINGS TPRI IN USEC

STEP INPUT RUN S14

C/AWN=1.00 R=61.5CM A=2.54CM D=7.97CM TMP=21DEGC

0.0	0.538	NOT RECORDED
7.00	-0.813	
19.0	0.869	
36.0	-0.875	
59.5	0.943	
89.2	-0.956	
120.0	1.000	
156.0	-0.863	
190.0	0.769	
235.0	-0.619	

STEP INPUT RUN S4

C/AWN=1.00 R=61.5CM A=1.00CM D=3.14CM TMP=20DEGC

0.0	0.176	0.80
1.25	-0.412	2.44
3.45	0.559	4.90
6.40	-0.598	8.75
10.5	0.696	13.3
16.0	-0.814	28.9
21.9	0.961	25.2
28.2	-1.000	32.4
35.7	1.000	40.5
45.2	-0.971	49.2
53.5	0.922	58.0
63.5	-0.863	68.5
74.0	0.784	79.0
85.0	-0.706	91.5
98.5	0.667	

DISPLACEMENT AXIS CROSSINGS TPRI IN USEC	DISPLACEMENT AMPLITUDES (NORMALIZED)	VELOCITY AXIS CROSSINGS TPRI IN USEC

STEP INPUT RUN S9
C/AWN=1.50 R=61.5CM A=1.00CM D=4.71CM TMP=21DEGC

0.0	0.307	1.30
2.30	-0.586	4.20
6.50	0.793	9.20
12.8	-0.923	16.5
20.6	1.000	25.0
30.6	-0.964	35.7
42.5	0.979	49.0
57.0	-0.943	65.0
71.5	0.821	79.0
88.0	-0.686	98.0
107.0	0.750	116.0
125.0	-0.700	135.0
145.0	0.593	154.0
169.0	-0.543	178.0
191.0	0.521	202.0
217.0	-0.543	225.0
239.0	0.564	246.0
262.0	-0.479	269.0
286.0	0.486	297.0
312.0		

STEP INPUT RUN S5
C/AWN=2.00 R=61.5CM A=1.00CM D=6.28CM TMP=20DEGC

0.0	0.351	2.10
3.80	-0.649	7.60
11.3	1.000	15.5
21.1	-1.000	26.2
34.4	0.979	41.0
52.5	-0.918	59.5
72.5	0.907	79.5
95.5	-0.701	101.0
119.0	0.731	127.0
145.0	-0.639	155.0
176.0	0.639	
203.0	-0.639	
235.0	0.639	
265.0	-0.598	
295.0	0.495	

DISPLACEMENT AXIS CROSSINGS TPRI IN USEC	DISPLACEMENT AMPLITUDES (NORMALIZED)	VELOCITY AXIS CROSSINGS TPRI IN USEC

STEP INPUT RUN S7
C/AWN=3.00 R=61.5CM A=1.00CM D=9.42CM TMP=20DEGC

0.0	0.432	4.50
7.50	-0.892	15.0
21.0	1.000	31.0
40.5	-0.826	53.0
67.0	0.822	84.5
100.0	-0.784	115.0
132.0	0.526	150.0
184.0	-0.427	210.0
222.0	0.376	
272.0	-0.319	
312.0	0.639	

VELOCITY AXIS CROSSINGS TPRI IN USEC	VELOCITY AMPLITUDES (NORMALIZED)

GATED SINE INPUT RUN G1 W=583.3KHZ
C/AWN=1.00 R=61.5CM A=2.54CM D=7.97CM TMP=20DEG

3.80	0.279
9.60	-0.669
15.9	1.000
21.5	-0.961
26.3	0.747
31.9	-0.870
37.0	0.851
42.2	-0.792
47.9	0.909
53.0	-0.870
58.5	0.857
63.5	-0.929
69.0	0.864
75.0	-0.909
79.5	0.870
84.5	-0.877
89.5	0.922
95.0	-0.864
100.5	0.916
105.0	-0.877
115.5	0.890
120.5	-0.883
125.5	0.857
131.0	-0.896
136.5	0.864
141.5	-0.877
147.0	0.883
152.5	-0.857
157.5	0.896
164.0	-0.831
172.5	

APPENDIX C PROGRAM STEPINS2

```
-COOP,,MILLERAC,0/49/S/1S/2S/E/45=54,30,30000,4.
-FTN,L,E.
      PROGRAM STEPINS2
C
C
C     THIS PROGRAM GIVES GRAPHS OF THE ACOUSTIC PRESSURE(PNRAT),PARTICLE
C     VELOCITY(VNRAT),AND PARTICLE DISPLACEMENT(ZNRAT) AT A POSITION
C     (R-A)METERS FROM A SOURCE OF RADIUS A METERS IN A PRESSURE RELEASE
C     ISO-VELOCITY LAYER OF DEPTH D METERS AS A RESULT OF A STEP INPUT
C     IN VELOCITY AT R-A=0 AT TIME T=0.
C
C
C     THESE ACOUSTIC VARIABLES ARE OBTAINED BY EVALUATING COMBINATIONS
C     OF TRUNCATED INFINITE SUMS OF BESSEL FUNCTIONS.PNRAT,VNRAT,AND
C     ZNRAT ARE EACH MADE UP OF A MAIN TERM(PN,VN,AND ZNMAIN) AND A
C     CORRECTION TERM(PN,VN,AND ZNCOR).GRAPHS OF THESE TERMS ARE
C     PRODUCED IN THE PROCESS OF EVALUATING PN,VN,AND ZNRAT.
C     AXIS CROSSINGS OF ALL MAIN AND RAT TERMS ARE CALUCATED.  THE
C     MAXIMA(POSITIVE OR NEGATIVE) OF ZNRAT(ZNRATM) AND TPRI OF THESE
C     MAXIMA(TPRIM) ARE DETERMINED.
C
C
C     INPUT DATA
C
C
C     DATA FIELDS        DATA DESCRIPTION(ALL MKS UNITS)
C
C     ALL E10.5          R=DISTANCE FROM PROBE TO CENTER OF SOURCE.
C                        A=RADIUS OF SOURCE
C
C                        DELT=INCREMENT OF TIME BY WHICH VALUES ARE
C                             GENERATED.
C
```

```
C                         TPMAX=MAXIMUM DELAYED TIME FOR WHICH VALUES
C                              ARE GENERATED.
C
C                         C=SPEED OF SOUND IN LAYER.
C
C                         EN=NORMAL MODE NUMBER OF THE LAYER CONTRIBUTING
C                              TO VALUES.
C
C                         D=DEPTH OF WATER IN LAYER.
C
C     I3,7X,7E10.0/(8E10.0).   FORMAT FOR EXPERIMENTAL DATA.  I3 IS
C                             FORMAT FOR N1, N2, N3, AND N4 EXPLAINED
C                             BELOW.  7X SKIPS TO COLUMN 11 AND REMAINING
C                             FIELDS ON AS MANY CARDS AS ARE NEEDED FOR
C                             EXPERIMENTAL DATA ARE E10.0.
C
C                         N1=NUMBER OF EXPERIMENTAL AXIS CROSSINGS IN
C                            PRESSURE.
C
C                         ACXP=EXPERIMENTALLY DETERMINED AXIS CROSSINGS
C                               IN PRESSURE.
C
C                         N2=NUMBER OF EXPERIMENTAL AXIS CROSSINGS IN
C                         VELOCITY.
C
C                         ACXV=EXPERIMENTALLY DETERMINED AXIS CROSSINGS
C                              IN VELOCITY.
C
C                         N3=NUMBER OF EXPERIMENTAL AXIS CROSSINGS IN
C                            DISPLACEMENT.
C
C                         ACXZ=EXPERIMENTALLY DETERMINED AXIS CROSSINGS
C                              IN DISPLACEMENT.
C
C                         N4=NUMBER OF EXPERIMENTAL MAXIMA(POSITIVE OR
C                            NEGATIVE) IN DISPLACEMENT.
```

```
C
C                           AMPXZ=EXPERIMENTALLY DETERMINED VALUES OF PEAK
C                                AMPLITUDES(POSITIVE OR NEGATIVE)IN
C                                PARTICLE DISPLACEMENT.
C
C
C     ØTHER VALUES
C
C
C     CPT=TIME OF FLIGHT OF SOUND FROM SOURCE TO PROBE AT POSITION R.
C
C     WN=CUT OFF FREQUENCY OF MODE NUMBER EN.
C
C     TPRI=DELAYED TIME.THE TIME WHICH HAS ELAPSED AT A POSITION R
C          SINCE THE TRANSIENT FIRST REACHED THAT POINT.TPRI WILL RUN
C          FROM 0 TO TPMAX IN INCREMENTS OF DELT.
C
C     S=DUMMY QUANTITY FOR CALL BES SUBROUTINE.
C
C     ARG=ARGUMENT OF BESSEL FUNCTIONS.
C
C     TVAL=((T-CPT/(T+CPT)).
C
C     PNRAT=TOTAL  ACOUSTIC PRESSURE.
C
C     PNMAIN=LEADING TERM OF EXPRESSION USED TO EVALUATE PNRAT. SEE
C     STATEMENT 301.
C
C     PNCOR=CORRECTION TERM IN PNRAT. SEE STATEMENT 301.
C
C     RESULT=VALUE CALL BES SUBROUTINE GIVES IN CALCULATING PNRAT. SEE
C     STATEMENT 4.
C
C     VNRAT=TOTAL PARTICLE VELOCITY. SEE STATEMENT 610
C
C     VNMAIN=FIRST TWO TERMS OF EXPRESSION USE TO EVALUATE VNRAT.  SEE
```

```
C       STATEMENT 610.
C
C       VNCOR=CORRECTION TERM IN VNRAT. SEE STATEMENT 601
C
C       ARESUL=VALUE CALL BES SUBROUTINE GIVES IN CALCULATING VNMAIN.
C       SEE STATEMENT 8.
C
C       BRESUL=VALUE CALL BES SUBROUTINE GIVES IN CALCULATING VNCOR. SEE
C       STATEMENT 11.
C
C       CRESUL=VALUE CALL BES SUBROUTINE GIVES IN CALCULATING ZNMAIN. SEE
C       STATEMENT 15
C
C       DRESUL=VALUE CALL BES SUBROUTINE GIVES IN CALCULATING ZNCOR.SEE
C       STATEMENT 18.
C
C       ZNRAT=TOTAL PARTICLE DISPLACEMENT.SEE STATEMENT 143.
C
C       ZNMAIN=LEADING TERM IN ZNRAT. SEE STATEMENT 143.
C
C       ZNCOR=CORRECTION TERM IN ZNRAT.SEE STATEMENT 143.
C
C       IT=ITITLE FOR CALL DRAW.
C
C       ACOPM=COMPUTED AXIS CROSSING IN PNRAT. SEE 1 STATEMENT PAST 601
C
C       ACOVM=COMPUTED AXIS CROSSING IN VNMAIN. SEE STATEMENT 101.
C
C       ACOVR=COMPUTED AXIS CROSSING IN VNRAT. SEE STATEMENT 141.
C
C       ACOZM=COMPUTED AXIS CROSSING IN ZNMAIN. SEE STATEMENT 171.
C
C       ACOZR=COMPUTED AXIS CROSSING IN ZNRAT. SEE STATEMENT 211.
C
C       ZNRATM=COMPUTED MAXIMA(POSITIVE OR NEGATIVE) OF ZNRAT. SEE
C       STATEMENT 2130.
```

```
C
C     AMPRAT=AMPXZ/ZNRATM. SEE 1 STATEMENT BEFORE 216.
C
C     TPRIM=TPRI OF ZNRATM.
C
C     A MAXIMUM OF 900 POINTS WILL BE CALCULATED AND PLOTTED.
C
C     THE LIBRARY ROUTINE   BES  IS USED IN THIS PROGRAM TO
C     EVALUATE ALL BESSEL FUNCTIONS USED. AS OF MARCH 1967 IT IS
C     LIBRARY ROUTINE   C3 BES. A COPY OF THIS ROUTINE  IS INCLUDED IN
C     THIS PROGRAM DECK.
C
C
      DIMENSION S(500),ARG(900),TPRI(900),TVAL(900),PNRAT(900),
     1PNCOR(900),PNMAIN(900),ARESUL(900),BRESUL(900),VNMAIN(900),
     2VNCOR(900),VNRAT(900),CRESUL(900),DRESUL(900),ZNCOR(900),
     3ZNRAT(900),ZNMAIN(900),RESULT(900),IT(12),ACOPM(30),ACOPR(30),
     4ACOVM(30),ACOVR(30),ACOZM(30),ACOZR(30),AMPXZ(30),ZNRATM(30),
     5AMPRAT(30),ACXP(30),ACXV(30),ACXZ(30),TPRIM(30)
    1 JJ=
      MAXCT=0
      ISIGN =0
      KK=
      READ 2,R,A,DELT,TPMAX,C,EN,D
    2 FORMAT(7E10.5)
      IF(DELT)200,200,201
  200 STOP
  201 CPT=(R-A)/C
      DOVERA=D/A
      WN=3.1415927*EN*C/D
      TN=6.2831854/WN
      CAWN=C/(A*WN)
      I=1
      TPRI(I)=0
    3 TVAL(I)=SQRTF(TPRI(I)/(TPRI(I)+2.*CPT))
      ARG(I)=WN*TPRI(I)/TVAL(I)
```

```
C
C
C 301 THIS PORTION EVALUATES PNRAT,PNMAIN,AND PNCOR FROM THE FOLLOWING
C     EXPRESSION,
C
C     PNRAT/(RHO*C)=JSUB O(ARG)-3/4*(C/(A*WN))*(1-A/R)*SUM(M=1 T/ 8)
C                           (-1)**(M-1)*((T-CPT)/(T+CPT))**((2M-1)/2)*
C                           JSUB(2M-1)(ARG)
C                           WHERE  ARG=WN*SQRTF(T**2-CPT**2)
C                                  JSUBO(ARG)=PNMAIN AND REMAINDER =
C                                  PNCOR.
C     IT ALSO DETERMINES IF AN AXIS CROSSING HAS OCCURRED IN PNMAIN OR
C     PNRAT TERM. IF SO,IT DETERMINES TPRI AT WHICH IT OCCURRED.
C
C
      JO=16
      TEMP=TVAL(I)
    4 CALL BES(JO,ARG(I),0,RESULT(I),S)
      PNMAIN(I)=S(1)
      AXCROSPM=PNMAIN(I)*PNMAIN(I-1)
      IF(AXCROSPM)41,42,42
   41 JJ=JJ+1
      ACOPM(JJ)=ABSF(PNMAIN(I-1))/(ABSF(PNMAIN(I-1))+ABSF(PNMAIN(I)))*
     1DELT+TPRI(I-1)
   42 CONTINUE
      SUM=TEMP*S(2)
      TEMP2=TEMP**2
    5 DO 6 J=4,JO,2
      TEMP=-TEMP*TEMP2
      SUM=SUM+TEMP*S(J)
    6 CONTINUE
      CORFACPN=3./4.*1.*CAWN*(1.+A/(3.*R))
      PNCOR(I)=CORFACPN*SUM
   60 PNRAT(I)=PNMAIN(I)-PNCOR(I)
      AXCROSPR=PNRAT(I)*PNRAT(I-1)
      IF(AXCROSPR)601,602,602
```

```
  601 KK=KK+1
      ACOPR(KK)=ABSF(PNRAT(I-1))/(ABSF(PNRAT(I-1))+ABSF(PNRAT(I)))*
     1DELT+TPRI(I-1)
  602 CONTINUE
C
C
C 610 THIS PORTION EVALUATES VNRAT,VNMAIN,AND VNCOR FROM THE FOLLOWING
C     EXPRESSION,
C
C     VNRAT=JSUB 0(ARG)+2*SUM(M=1 TO 10)((T-CPT)/(T+CPT))**M*JSUB 2M
C            (ARG)-3/4*(C/(A*WN))*(1-A/R)*SUM(M=1 TO 11)((T-CPT)/(T+CPT))**
C              ((2M-1)/2)*JSUB(2M-1)(ARG)
C                               WHERE THE FIRST TWO TERMS = VNMAIN AND
C                               THE THIRD TERM=VNCOR.ARG IS SAME AS BEFORE.
C     IT ALSO DETERMINES IF AN AXIS CROSSING HAS OCCURRED IN VNMAIN OR
C     VNRAT TERM. IF SO,IT DETERMINES TPRI AT WHICH IT OCCURRED.
C
C
    7 KO=22
      ATEMP=TVAL(I)**2
    8 CALL BES(KO,ARG(I),0,ARESUL(I),S)
      ASUM=ATEMP*S(3)
      TEMP=ATEMP
    9 DO 10 K=5,KO,2
      TEMP=ATEMP*TEMP
      ASUM=ASUM+TEMP*S(K)
   10 CONTINUE
      VNMAIN(I)=PNMAIN(I)+2.*ASUM
      AXCROSVM=VNMAIN(I)*VNMAIN(I-1)
      IF(AXCROSVM)101,102,102
  101 ACOVM(JJ)=ABSF(VNMAIN(I-1))/(ABSF(VNMAIN(I-1))+ABSF(VNMAIN(I)))*
     1DELT+TPRI(I-1)
  102 CONTINUE
      LO=22
      TEMP=TVAL(I)
   11 CALL BES(LO,ARG(I),0,BRESUL(I),S)
```

```
      BSUM=TEMP*S(2)
      TEMP2=TEMP**2
   12 DO 13 L=4,LO,2
      TEMP=TEMP*TEMP2
      BSUM=BSUM+TEMP*S(L)
   13 CONTINUE
      CORFACVN=3./4.*1.*CAWN*(1.-A/R)
      VNCOR(I)=CORFACVN*BSUM
   14 VNRAT(I)=VNMAIN(I)-VNCOR(I)
      AXCROSVR=VNRAT(I)*VNRAT(I-1)
      IF(AXCROSVR)141,142,142
  141 ACOVR(KK)=ABSF(VNRAT(I-1))/(ABSF(VNRAT(I-1))+ABSF(VNRAT(I)))*
     1DELT+TPRI(I-1)
  142 CONTINUE
C
C
C 143 THIS PORTION EVALUATES ZNRAT,ZNMAIN,AND ZNCOR FROM THE FOLLOWING
C     EXPRESSION,
C
C     ZNRAT/(2/WN)=SUM(M=1 TO 8)(2M-1)*((T-CPT)/(T+CPT))**((2M-1)/2)*
C                  JSUB(2M-1)(ARG)-3/4*(C/(A*WN))*(1-A/R)*SUM(M= 1 TO 7)M*
C                  ((T-CPT)/(T+CPT))**M*JSUB 2M(ARG)
C
C                              WHERE THE FIRST TERM IS ZNMAIN,SECOND TERM
C                              IS ZNCOR,AND ARG IS SAME AS BEFORE.
C     IT ALSO DETERMINES IF AN AXIS CROSSING HAS OCCURRED IN ZNMAIN OR
C     ZNRAT TERM. IF SO,IT DETERMINES TPRI AT WHICH IT OCCURRED.
C
C
      MO=16
      TEMP=TVAL(I)
   15 CALL BES(MO,ARG(I),0,CRESUL(I),S)
      CSUM=TEMP*S(2)
      TEMP2=TEMP**2
   16 DO 17 M=4,MO,2
      TEMP=TEMP*TEMP2
```

```
      CSUM=CSUM+(M-1)*TEMP*S(M)
   17 CONTINUE
      ZNMAIN(I)=CSUM
      AXCROSZM=ZNMAIN(I)*ZNMAIN(I-1)
      IF(AXCROSZM)171,172,172
  171 ACOZM(JJ)=ABSF(ZNMAIN(I-1))/(ABSF(ZNMAIN(I-1))+ABSF(ZNMAIN(I)))*
     1DELT+TPRI(I-1)
  172 CONTINUE
      NO=14
      DTEMP=TVAL(I)**2
   18 CALL BES(NO,ARG(I),0,DRESUL(I),S)
      DSUM=DTEMP*S(3)
      TEMP=DTEMP
   19 DO 20 N=5,NO,2
      TEMP=TEMP*DTEMP
      DSUM=DSUM+(N-1)/2.*TEMP*S(N)
   20 CONTINUE
      CORFACZN=3./4.*1.*CAWN*(1.-A/R)
      ZNCOR(I)=CORFACZN*DSUM
   21 ZNRAT(I)=ZNMAIN(I)-ZNCOR(I)
      AXCROSZR=ZNRAT(I)*ZNRAT(I-1)
      IF(AXCROSZR)211,212,212
  211 ACOZR(KK)=ABSF(ZNRAT(I-1))/(ABSF(ZNRAT(I-1))+ABSF(ZNRAT(I)))*
     1DELT+TPRI(I-1)
  212 CONTINUE
C
C
C     THIS PORTION DETERMINES THE MAXIMA (POSITIVE OR NEGATIVE) OF
C     ZNRAT(ZNRATM) AND THE TPRI OF THESE MAXIMA(TPRIM).
C
C
 2130 IF(ZNRAT(I-1)-ZNRAT(I)) 2140,2160,2160
 2140 IF(ISIGN) 2180,2150,2190
 2150 IF(I-1) 2190,2190,2155
 2155 ISIGN=+1
      GO TO 2190
```

```
 2160 IF(ISIGN) 2190,2170,2180
 2170 IF(I-1) 2190,2190,2175
 2175 ISIGN=-1
      GO TO 2190
 2180 MAXCT=MAXCT+1
      ZNRATM(MAXCT)=ABSF(ZNRAT(I-1))
      TPRIM(MAXCT)=TPRI(I-1)
      ISIGN=-ISIGN
 2190 CONTINUE
      IF(I-900) 22,23,23
   22 I=I+1
      TPRI(I)=TPRI(I-1)+DELT
      NN=I-1
      IF(TPRI(I)-TPMAX)3,3,23
   23 CALL NORM(ZNRATM,MAXCT)
C
C
C     THIS PORTION READS IN THE EXPERIMENTAL DATA AND CALCULATES AMPRAT
C
C
      READ 215,N1,(ACXP(JJ),JJ=1,N1)
  215 FORMAT(I3,7X,7E10.0/(8E10.0))
      READ 215,N2,(ACXV(JJ),JJ=1,N2)
      READ 215,N3,(ACXZ(JJ),JJ=1,N3)
      READ 215,N4,(AMPXZ(JJ),JJ=1,N4)
      CALL NORM(AMPXZ,N4)
      DO 216 M2=1,N4
      AMPRAT(M2)=AMPXZ(M2)/ZNRATM(M2)
  216 CONTINUE
C
C
C     PRINT OUT PORTION OF PROGRAM
C
C
      PRINT 24,R,A,EN,D,C,TN,DOVERA,WN,CAWN,CORFACPN,CORFACVN,CORFACZN
   24 FORMAT(4H1R =,E10.5,4H A =,E10.5,5H EN =,E10.5,4H D =,E10.5,
```

```
      14H C =,E10.5,5H TN =,E10.5,9H DOVERA =,E10.5,//5H WN =,E10.5,
      27H CAWN =,E10.5,11H CORFACPN =,E10.5,11H CORFACVN =,E10.5,
      311H CORFACZN =,E10.5)
   25 PRINT 26,(I,TPRI(I),ARG(I),PNMAIN(I),PNCOR(I),PNRAT(I),I=1,NN)
   26 FORMAT(1H0,17X,4HTPRI,13X,3HARG,14X,6HPNMAIN,18X,5HPNCOR,16X,
      15HPNRAT,//(1X,I4,5E20.8))
   27 PRINT 28,(I,TPRI(I),ARG(I),VNMAIN(I),VNCOR(I),VNRAT(I),I=1,NN)
   28 FORMAT(1H0,17X,4HTPRI,14X,3HARG,14X,6HVNMAIN,16X,5HVNCOR,16X,
      15HVNRAT,//(1X,I4,5E20.8))
   29 PRINT 30,(I,TPRI(I),ARG(I),ZNMAIN(I),ZNCOR(I),ZNRAT(I),I=1,NN)
   30 FORMAT(1H0,17X,4HTPRI,14X,3HARG,14X,6HZNMAIN,16X,5HZNCOR,16X,
      15HZNRAT,//(1X,I4,5E20.8))
      PRINT 32,(I,ACOPR(I),ACOPM(I),ACXP(I),I,I=1,N1)
   32 FORMAT(1H0,17X,5HACOPR,13X,5HACOPM,16X,4HACXP,//
      1(1X,I4,3E20.8,I4))
      PRINT 33,(I,ACOVR(I),ACOVM(I),ACXV(I),I,I=1,N2)
   33 FORMAT(1H0,17X,5HACOVR,13X,5HACOVM,16X,4HACXV,//
      1(1X,I4,3E20.8,I4))
      PRINT 34,(I,ACOZR(I),ACOZM(I),ACXZ(I),I,I=1,N3)
   34 FORMAT(1H0,17X,5HACOZR,13X,5HACOZM,16X,4HACXZ,//
      1(1X,I4,3E20.8,I4))
      PRINT 35,(I,ZNRATM(I),AMPXZ(I),AMPRAT(I),TPRIM(I),I,I=1,N4)
   35 FORMAT(1H0,16X,6HZNRATM,12X,5HAMPXZ,14X,6HAMPRAT,15X,5HTPRIM,//
      1(1X,I4,4E20.8,I4))
C
C
C     GRAPH PLOTTING PORTION OF PROGRAM
C
C
      READ 40,IT
   40 FORMAT(6A8)
      CALL DRAW(NN,TPRI,PNRAT,0,0,4H    ,IT,0,0,0,0,0,0,9,15,0,LAST)
      READ 40,IT
      CALL DRAW(NN,TPRI,PNMAIN,0,0,4H    ,IT,0,0,0,0,0,0,9,15,0,LAST)
      READ 40,IT
      CALL DRAW(NN,TPRI,PNCOR,0,0,4H    ,IT,0,0,0,0,0,0,9,15,0,LAST)
```

```
      READ 40,IT
      CALL DRAW(NN,TPRI,VNRAT,0,0,4H    ,IT,0,0,0,0,0,0,9,15,0,LAST)
      READ 40,IT
      CALL DRAW(NN,TPRI,VNMAIN,0,0,4H    ,IT,0,0,0,0,0,0,9,15,0,LAST)
      READ 40,IT
      CALL DRAW(NN,TPRI,VNCOR,0,0,4H    ,IT,0,0,0,0,0,0,9,15,0,LAST)
      READ 40,IT
      CALL DRAW(NN,TPRI,ZNRAT,0,0,4H    ,IT,0,0,0,0,0,0,9,15,0,LAST)
      READ 40,IT
      CALL DRAW(NN,TPRI,ZNMAIN,0,0,4H    ,IT,0,0,0,0,0,0,9,15,0,LAST)
      READ 40,IT
      CALL DRAW(NN,TPRI,ZNCOR,0,0,4H    ,IT,0,0,0,0,0,0,9,15,0,LAST)
      READ 40,IT
      CALL DRAW(N4,TPRIM,AMPRAT,0,5,8H        ,IT,6.0E-05,0,0,0,0,0,6,
     13,0,LAST)
      READ 40,IT
      CALL DRAW(N3,ACOZM,ACXZ,0,1,8H        ,IT,0,0,0,0,0,0,5,5,0,LAST)
      READ 40,IT
      CALL DRAW(N3,ACOZR,ACXZ,0,1,8H        ,IT,0,0,0,0,0,0,5,5,0,LAST)
      GO TO 1
      END
      SUBROUTINE BES(NO,X,KODE,RESULT,T)                                0000000
      DIMENSION T(500)
107   FORMAT(55H1NEGATIVE ORDER NOT ACCEPTED IN BESSEL FUNCTION ROUTINE)00000020
      KO=NO+1                                                           0000  3
      IF(X) 6,1,6                                                       00000 4
1     IF(NO) 4,2,3                                                      0000005
2     T(1 )=1.0                                                           00006
      RESULT=1.0                                                        0000  7
      RETURN                                                            0000  8
4     IF(KO) 5,10,3                                                     0000009
3     RESULT=0                                                          0000010
      T(1)=0.                                                             00011
      RETURN                                                            0000012
10    RESULT=9.999999999E200                                            0000013
      RETURN                                                            0000014
```

```
5      PRINT 107
      STOP1
6     IF(NO) 5,7,7
    7 JO=2*XFIXF(X)
      MO=NO
      IF(MO-JO) 11,12,12
11    MO=JO
12    MO=MO+11
      T(MO)=0.
      LUB=MO-1
      T(LUB)=1.0E-300
      IF(KODE) 51,23,51
23    F=2*LUB
      MO=MO-3
      I2=MO
24    F=F 2.
      T(I2+1)=F/X*T(I2+2)-T(I2+3)
      IF(I2)25,26,25
25    I2=I2-1
      GO TO 24
26    SUM=T(1)
      DO4  J=3,MO,2
40    SUM=SUM+2.*T(J)
      F=1./SUM
      DO 50 J= 1,KO
50    T(J)=T(J)*F
      RESULT=T(KO)
      RETURN
51    F=2*LUB-2
      MO=MO-3
      I2=MO
511   T(I2+1)=F/X*T(I2+2)+T(I2+3)
      IF(I2)52,53,52
52    I2=I2-1
      F=F 2.
      GO TO 511
```

```
53    SUM=T(1)
      DO 70 J=2,MO
70    SUM=SUM+2.*T(J)
      F=1./(SUM*EXPF(X))
      DO 80 J=1,KO
80    T(J)=T(J)*F
      RESULT=T(KO)
      RETURN
      END
      SUBROUTINE NORM(A,N)
      DIMENSION A(N)
      J=1
      DO 10 I=1,N
      IF (ABSF(A(J))-ABSF(A(I))) 5,10,10
    5 J=I
   10 CONTINUE
      TEMP=A(J)
      DO 20 I=1,N
   20 A(I)=A(I)/TEMP
      RETURN
      END
      END
         FINIS
-EXECUTE.
C
C     SAMPLE DATA DECK FOR ONE RUN.(THIS CARD DOES NOT GO INTO THE
C     PROGRAM).  LAST CARD OF DATA DECK MUST BE A BLANK CARD.
C
  6.15E-01  2.54E-02   4.0E-07  3.60E-041.48266E03   1.00E00  5.50E-02
 12         1.70E-06  5.10E-06  12.7E-06                      53.0E-06  72.0E-06
 94.0E-06  11.3E-05  13.6E-05  16.7E-05  18.8E-05
 12         2.20E-06  6.70E-06  14.4E-06  23.2E-06  38.6E-06  52.5E-06  73.5E-06
 93.0E-06  11.9E-05  14.0E-05  16.9E-05  19.3E-05
 17         3.50E-06  9.60E-06  18.4E-06  29.8E-06  45.8E-06  64.0E-06  85.0E-06
 10.6E-05  13.1E-05  16.8E-05  18.3E-05  21.2E-05  24.0E-05  26.8E-05  29.8E-05
 32.9E-05  36.0E-05
```

```
 17          .410E0   0.680E0   0.980E0    .990E0   0.910E0   0.900E0   0.820E0
   0.845E    .790E0   0.720E0   0.760E0    .680E0   0.680E0   0.650E0   0.660E0
   0.575E    .610E0
MILLER BOX M PNRAT VS TPRI  DELT=.4US TPMAX=360US
R=.615M A=.0254M D=.055M C=1482.66M/SEC  4/06/67
MILLER BOX M PNMAIN VS TPRI  DELT=.4U TPMAX=360US
R=.615M A=.0254M D=.055M C=1482.66M/SEC  4/06/67
MILLER BOX M PNCOR VS TPRI  DELT=.4US TPMAX=360US
R=.615M A=.0254M D=.055M C=1482.66M/SEC  4/06/67
MILLER BOX M VNRAT VS TPRI  DELT=.4US TPMAX=360US
R=.615M A=.0254M D=.055M C=1482.66M/SEC  4/06/67
MILLER BOX M VNMAIN VS TPRI  DELT=.4U TPMAX=360US
R=.615M A=.0254M D=.055M C=1482.66M/SEC  4/06/67
MILLER BOX M VNCOR VS TPRI  DELT=.4US TPMAX=360US
R=.615M A=.0254M D=.055M C=1482.66M/SEC  4/06/67
MILLER BOX M ZNRAT VS TPRI  DELT=.4US TPMAX=360US
R=.615M A=.0254M D=.055M C=1482.66M/SEC  4/06/67
MILLER BOX M ZNMAIN VS TPRI  DELT=.4U TPMAX=360US
R=.615M A=.0254M D=.055M C=1482.66M/SEC  4/06/67
MILLER BOX M ZNCOR VS TPRI  DELT=.4US TPMAX=360US
R=.615M A=.0254M D=.055M C=1482.66M/SEC  4/06/67
        NORM AMPRAT VS TPRI CAWN = 0.69 5/5/67

MILLER BOX M ACXZ VS ACOZM D/A=2.17      4/13/67

MILLER BOX M ACXZ VS ACOZR D/A=2.17      4/13/67
```

APPENDIX D PROGRAM GATEINS2

```
-COOP,,MILLERAC,0/49/S/1S/2S/E/45=54,10,30000,4.
-FTN,L,E.
      PROGRAM GATEINS2
C
C
C     THIS PROGRAM GIVES A GRAPH OF THE PARTICLE VELOCITY (VNRAT) AT A
C     POSITION (R-A) METERS FROM A SOURCE OF RADIUS A METERS LOCATED AT
C     R=0 IN A PRESSURE RELEASE CHANNEL OF DEPTH D METERS AS A RESULT OF
C     A GATED SIGN WAVE INPUT OF FREQUENCY F AT T=0.
C
C     THE PARTICLE VELOCITY IS OBTAINED BY EVALUATING COMBINATIONS OF
C     LOMMEL FUNCTIONS.  VNRAT IS MADE UP OF A MAIN TERM(VNMAIN) AND A
C     CORRECTION TERM(VNCOR).  PRINT OUT AND GRAPHS OF THESE TERMS ARE
C     PRODUCED IN THE PROCESS OF EVALUATING VNRAT.
C
C
C     INPUT DATA
C
C
C     DATA FIELDS       DATA DESCRIPTION(ALL MKS UNITS)
C
C      8E10.5           R=DISTANCE FROM PROBE TO CENTER OF SOURCE.
C
C                       A=RADIUS OF SOURCE.
C
C                       DELT=INCREMENT OF TIME BY WHICH PARTICLE VELOCITY
C                            IS GENERATED.
C
C                       TPMAX=MAXIMUM DELAYED TIME FOR WHICH PARTICLE
C                             VELOCITY IS GENERATED.
C
C                       C=SPEED OF SOUND IN THE CHANNEL.
C
```

```
C                         EN=NORMAL MODE NUMBER OF THE CHANNEL CONTRIBUTING TO
C                            THE PARTICLE VELOCITY.
C
C                         D=DEPTH OF WATER IN THE CHANNEL.
C
C                         F=FREQUENCY OF GATED SINE WAVE INPUT.
C
C
C     I3,7X,7E10.0/       FORMAT FOR EXPERIMENTAL DATA.  I3,7X,7E10.0 IS
C     (8E10.0)            FOR FIRST CARD, WITH I3 FOR N2 AND N4 EXPLAINED
C                         BELOW.  7X SKIPS TO COLUMN 11.  REMAINING 7E10.0
C                         IS FOR DATA AS ARE SUBSEQUENT CARDS(8E10.0).
C
C                          N2=NUMBER OF EXPERIMENTAL AXIS CROSSINGS IN
C                             VELOCITY.
C
C                          ACXV=EXPERIMENTALLY DETERMINED AXIS CROSSINGS
C                               IN VELOCITY.
C
C                          N4=NUMBER OF EXPERIMENTAL MAXIMA(POSITIVE OR
C                             NEGATIVE) IN VELOCITY.
C
C                          AMPXV=EXPERIMENTALLY DETERMINED VALUES OF PEAK
C                                AMPLITUDES(POSITIVE OR NEGATIVE) IN
C                                PARTICLE VELOCITY.
C
C
C     ΘTHER VALUES
C
C
C     CPT=TIME OF FLIGHT OF SOUND FROM SOURCE TO PROBE AT POSITION R.
C
C     TPRI=DELAYED TIME.THE TIME WHICH HAS ELAPSED AT A POSITION R
C          SINCE THE TRANSIENT FIRST REACHED THAT POINT.TPRI WILL RUN
C          FROM 0 TO TPMAX IN INCREMENTS OF DELT.
C
```

```
C       Z=FIRST OF TWO ARGUMENTS OF LOMMEL FUNCTIONS USED.  APPEARS WHEN
C         CALLING FUNCTION LOMMEL.
C
C       XP,XM=SECOND OF TWO ARGUMENTS OF LOMMEL FUNCTIONS USED.  APPEARS
C             WHEN CALLING FUNCTION LOMMEL.
C
C       U1P,U1M,U0P,U0M=VALUES FUNCTION LOMMEL GIVES FOR U(Z,XP,1),
C                       U(Z,XM,1),U,Z,XP,0), AND U(Z,XM,0) RESPECTIVELY.
C                       HERE 1 AND 0 INDICATE ORDER OF LOMMEL FUNCTION
C                       EVALUATED.
C
C       ACOVR=COMPUTED AXIS CROSSING IN VNRAT. SEE STATEMENT 141.
C
C       ACOVM=COMPUTED AXIS CROSSING IN VNMAIN. SEE STATEMENT 101.
C
C       VNRATM=COMPUTED MAXIMA(POSITIVE OR NEGATIVE) OF VNRAT. SEE
C             STATEMENT 2130.
C
C       TPRIM=TPRI OF VNRATM.
C
C       WN=CUT OFF FREQUENCY OF MODE NUMBER EN.
C
C       IT=ITITLE FOR CALL DRAW.
C
C       A MAXIMUM OF 900 POINTS WILL BE CALCULATED AND PLOTTED.
C
C
        DIMENSION TPRI(900),VNRAT(900),VNMAIN(900),VNCOR(900),Z(900),
       1XP(900),XM(900),U1P(900),U1M(900),U0P(900),U0M(900),IT(12),
       2ALOM1(900),ALOM0(900),ACOVM(50),ACOVR(50),ACXV(50),AMPXV(50),
       3VNRATM(900),AMPRAT(50),TPRIM(50)
      1 JJ=
        KK=
        MAXCT=0
        ISIGN=0
        READ 2,R,A,DELT,TPMAX,C,EN,D,F
```

```
      IF(DELT) 10,11,10
    2 FORMAT(8E10.5)
   10 CPT=(R-A)/C
      W=2.*3.1417*F
      WN=3.1415927*EN*C/D
      RAD=SQRTF(1.0-(WN/W)**2)
      RAD2=SQRTF((W/WN)**2-1)
      CAWN=C/(A*WN)
      I=1
      TPRI(I)=0
C
C
C     THIS PORTION CALCULATES ARGUMENTS OF LOMMEL FUNCTIONS USED AND
C     EVALUATES THESE FUNCTIONS BY MEANS OF FUNCTION LOMMEL.
C
C
    3 XP(I)=W*TPRI(I)*(1.0+RAD)
      XM(I)=W*TPRI(I)*(1.0-RAD)
      Z(I)=WN*TPRI(I)*SQRTF(1.0+2.0*CPT/TPRI(I))
      U1P(I)=U(Z(I),XP(I),1)
      U1M(I)=U(Z(I),XM(I),1)
      U0P(I)=U(Z(I),XP(I),0)
      U0M(I)=U(Z(I),XM(I),0)
      ALOM1(I)=U1P(I)+U1M(I)
      ALOM0(I)=U0P(I)-U0M(I)
C
C
C     THIS PORTION EVALUATES VNMAIN, VNCOR, AND VNRAT AND FINDS TPRI OF
C     ANY AXIS CROSSINGS IN VNMAIN OR VNRAT.
C
C
      VNMAIN(I)=ALOM1(I)
      AXCROSVM=VNMAIN(I)*VNMAIN(I-1)
      IF(AXCROSVM)101,102,102
  101 JJ=JJ+1
      ACOVM(JJ)=ABSF(VNMAIN(I-1))/(ABSF(VNMAIN(I-1))+ABSF(VNMAIN(I)))*
```

```
   1DELT+TPRI(I-1)
 102 CONTINUE
     CORFACVN=3./8.*(1-(A/R))*CAWN/RAD2
     VNCOR(I)=CORFACVN*ALOMO(I)
     VNRAT(I)=VNMAIN(I)+VNCOR(I)
     AXCROSVR=VNRAT(I)*VNRAT(I-1)
     IF(AXCROSVR)141,142,142
 141 KK=KK+1
     ACOVR(KK)=ABSF(VNRAT(I-1))/(ABSF(VNRAT(I-1))+ABSF(VNRAT(I)))*
    1DELT+TPRI(I-1)
 142 CONTINUE
C
C
C    THIS PORTION DETERMINES MAXIMA(POSITIVE OR NEGATIVE) OF VNRAT
C    (VNRAT)AND TPRI OF THESE MAXIMA(TPRIM).
C
C
2130 IF(VNRAT(I-1)-VNRAT(I)) 2140,2160,2160
2140 IF(ISIGN) 2180,2150,2190
2150 IF(I-1) 2190,2190,2155
2155 ISIGN=+1
     GO TO 2190
2160 IF(ISIGN) 2190,2170,2180
2170 IF(I-1) 2190,2190,2175
2175 ISIGN=-1
     GO TO 2190
2180 MAXCT=MAXCT+1
     VNRATM(MAXCT)=ABSF(VNRAT(I-1))
     TPRIM(MAXCT)=TPRI(I-1)
     ISIGN=-ISIGN
2190 CONTINUE
     IF(I-900)4,50,50
   4 I=I 1
     TPRI(I)=TPRI(I-1)+DELT
     J=I 1
     IF(TPRI(I)-TPMAX)3,3,5
```

```
   50 WRITE(51,60)I
   60 FORMAT(5X,2HI=,I5)
      CALL NORM(VNRATM,MAXCT)
C
C
C     THIS PORTION READS IN EXPERIMENTAL DATA AND CALCULATES AMPRAT.
C
C
    5 READ 215,N4,(AMPXV(JJ),JJ=1,N4)
  215 FORMAT(I3,7X,7E10.0/(8E10.0))
      CALL NORM(AMPXV,N4)
      DO 216 M2=1,N4
      AMPRAT(M2)=AMPXV(M2)/VNRATM(M2)
  216 CONTINUE
      READ 215,N2,(ACXV(JJ),JJ=1,N2)
C
C
C     PRINT OUT PORTION OF PROGRAM.
C
C
      PRINT 6,R,A,DELT,TPMAX,C,EN,D,F,WN,W,CAWN,CORFACVN
    6 FORMAT(4H1R =,E10.5,4H A =,E10.5,7H DELT =,E10.5,8H TPMAX =,E10.5,
     14H C =,E10.5,5H EN =,E10.5/4H D =,E10.5,4H F =,E10.5,5H WN =,
     2E10.5,4H W =,E10.5,7H CAWN =,E10.5,11H CORFACVN =,E10.5)
    7 PRINT 8,(I,TPRI(I),VNCOR(I),VNMAIN(I),VNRAT(I),I,I=1,J)
    8 FORMAT(1H0,11X,4HTPRI,14X,5HVNCOR,14X,6HVNMAIN,13X,5HVNRAT,//
     1(1X,I4,4E20.8,I4))
      PRINT 33,(I,ACOVR(I),ACOVM(I),ACXV(I),I,I=1,N2)
   33 FORMAT(1H0,17X,5HACOVR,13X,5HACOVM,16X,4HACXV,//
     1(1X,I4,3E20.8,I4))
      PRINT 35,(I,VNRATM(I),AMPXV(I),AMPRAT(I),TPRIM(I),I,I=1,N4)
   35 FORMAT(1H0,16X,6HVNRATM,12X,5HAMPXV,14X,6HAMPRAT,15X,5HTPRIM,//
     1(1X,I4,4E20.8,I4))
C
C
C     GRAPH PLOTTING PORTION OF PROGRAM.
```

```
      READ 40,IT
   40 FORMAT(6A8)
      CALL DRAW(J,TPRI,VNRAT,0,0,4H    ,IT,3.0E-05,1.0E0,0,0,0,0,6,6,
     10,LAST)
      READ 40,IT
      CALL DRAW(J,TPRI,VNMAIN,0,0,4H    ,IT,3.0E-05,1.0E0,0,0,0,0,6,6,
     10,LAST)
      READ 40,IT
      CALL DRAW(J,TPRI,VNCOR,0,0,4H    ,IT,3.0E-05,1.0E0,0,0,0,0,6,6,
     10,LAST)
      READ 40,IT
      CALL DRAW(N4,TPRIM,AMPRAT,0,5,8H        ,IT,6.0E-05,0,0,0,0,0,6,
     13,0,LAST)
      GO TO 1
   11 STOP
      END
      FUNCTION U(ZZ,XX,NN)
C
C
C
C
C    THIS FUNCTION COMPUTES THE VALUE OF THE NN TH ORDER OF  LOMMEL FUNCTIONS OF
C    TWΘ ARGUMENTS,USUB NN(ZZ,XX).  IN THIS PROGRAM THE MAGNITUDE OF  ZZ MUST BE
C    LESS THAN OR EQUAL TO 2000 TO CONSERVE STORAGE SPACE. THIS LIMITATION MAY BE
C    REMOVED IF DESIRED.  U IS EVALUATED AS DIFFERENT SUMS OF INFINITE SERIES OF
C    BESSEL FUNCTIONS DEPENDING ON THE RELATIVE MAGNITUDES OF ZZ AND XX, THIS IS
C    DONE TO ENSURE THE MOST RAPID CONVERGENCE OF THE SERIES USED.
C
C      IN THIS PROGRAM NN = 0 OR 1.
C
C    IF/XX/ IS LESS THAN OR EQUAL TO /ZZ/,
C
C         U=SUM N=1,INF OF (-1)**(N-1)*(XX/ZZ)**(2N-1)*JSUB2N-1(ZZ)
C
```

```
C   IF /XX/ IS GREATER THAN /ZZ/,
C
C        U=V+SIN(XX/2+ZZ**2/(2XX))
C                  WHERE V=SUM N=1,INF OF (-1)**N*(ZZ/XX)**(2N-1)*JSUB2N-1(ZZ).
C
C
C   IN BOTH CASES THE MAXIMUM VALUE OF N USED IN THE SUMMATION DEPENDS ON /ZZ/.
C
C        IF ZZ/2 IS LESS THAN XX IS LESS THAN 2ZZ,  N=20+1.2Z
C
C        OTHERWISE N=23.
C
C   THIS CRITERIA FOR N IS NECESSARY BECAUSE THE CONVERGENCE OF THE SERIE  IS
C   POOREST IN THE REGION ZZ/2 IS LESS THAN XX IS LESS THAN 2ZZ AND BECOMES
C   WORSE AS /ZZ/ INCREASES.
C
C
      COMMON/BESSEL/ NO,Z,KODE,RESULT,B(4000)
      Z=ZZ
      ARG=XX
      N=NN
      KODE=0
      IF(Z-2000.0) 120,120,100
  100 WRITE(51,2100) Z
 2100 FORMAT(21H0Z IS TOO LARGE, Z=   E2 .8)
      RETURN
  120 IF(ARG-Z) 200,200,220
  200 IF(ARG-Z*0.5) 205,205,203
  203 NO=20+XFIXF(Z*1.2)+N
      GO TO 208
  205 NO=23+N
  208 TEMP=ARG/Z
      CALL BES
      VAL=TEMP*B(N+1)
      TEMP2=TEMP**2
      MSTART=N+3
```

```
      DO 210 M=MSTART,NO,2
      TEMP=-TEMP*TEMP2
      VAL=VAL+TEMP*B(M)
  210 CONTINUE
      U=VAL
      RETURN
  220 IF(ARG-(Z+Z)) 225,230,230
  225 NO=20+XFIXF(Z*1.2)+N
      GO TO 235
  230 NO=23+N
  235 TEMP=-Z/ARG
      TEMP2=TEMP**2
      TEMP=TEMP**N
      CALL BES
      V=TEMP*B(N+1)
      MSTART=N+3
      DO 240 M=MSTART,NO,2
      TEMP=-TEMP*TEMP2
      V=V TEMP*B(M)
  240 CONTINUE
      IF(N)260,250,260
  250 U=B(1)-V+COSF(ARG/2.+Z*Z/(ARG+ARG))
      RETURN
  260 U=V SINF(ARG/2.0+Z**2/(ARG+ARG))
      RETURN
      END
      SUBROUTINE BES
      COMMON/BESSEL/ NO,X,KODE,RESULT,T(4000)
107   FORMAT(55H1NEGATIVE ORDER NOT ACCEPTED IN BESSEL FUNCTION ROUTINE)
      KO=NO+1
      IF(X) 6,1,6
1     IF(NO) 4,2,3
2     T(1 )=1.0
      RESULT=1.0
      RETURN
4     IF(KO) 5,10,3
```

```
3     RESULT=0
      T(1)=0.
      RETURN
10    RESULT=9.999999999E200
      RETURN
 5     PRINT 107
      STOP1
6     IF(NO) 5,7,7
    7 JO=2*XFIXF(X)
      MO=NO
      IF(MO-JO) 11,12,12
11    MO=JO
12    MO=MO+11
      T(MO)=0.
      LUB=MO-1
      T(LUB)=1.0E-300
      IF(KODE) 51,23,51
23    F=2*LUB
      MO=MO-3
      I2=MO
24    F=F 2.
      T(I2+1)=F/X*T(I2+2)-T(I2+3)
      IF(I2)25,26,25
25    I2=I2-1
      GO TO 24
26    SUM=T(1)
      DO4  J=3,MO,2
40    SUM=SUM+2.*T(J)
      F=1./SUM
      DO 50 J= 1,KO
50    T(J)=T(J)*F
      RESULT=T(KO)
      RETURN
51    F=2*LUB-2
      MO=MO-3
      I2=MO
```

```
 511  T(I2+1)=F/X*T(I2+2)+T(I2+3)
      IF(I2)52,53,52
 52   I2=I2-1
      F=F 2.
      GO TO 511
 53   SUM=T(1)
      DO 70 J=2,MO
 70   SUM=SUM+2.*T(J)
      F=1./(SUM*EXPF(X))
      DO 80 J=1,KO
 80   T(J)=T(J)*F
      RESULT=T(KO)
      RETURN
      END
      SUBROUTINE NORM(A,N)
      DIMENSION A(N)
      J=1
      DO 10 I=1,N
      IF (ABSF(A(J))-ABSF(A(I))) 5,10,10
    5 J=I
   10 CONTINUE
      TEMP=A(J)
      DO 20 I=1,N
   20 A(I)=A(I)/TEMP
      RETURN
      END
      END
         FINIS
-EXECUTE.
C
C
C     SAMPLE DATA DECK.  THIS CARD SHOULD NOT BE INCLUDED IN THE
C     PROGRAM.  THE LAST CARD OF THE DATA DECK MUST BE A BLANK CARD.
C
C
  6.15E-01  2.54E-02  2.00E-07  1.80E-041.47955E03   1.00E00  7.97E-02  92.84E03
```

```
30            2.15E-01  5.15E-01  7.70E-01  7.40E-01  5.75E-01  6.70E-01  6.55E-01
 6.10E-01  7.00E-01  6.70E-01  6.60E-01  7.15E-01  6.65E-01  7.00E-01  6.70E-01
 6.75E-01  7.10E-01  6.65E-01  7.05E-01  6.75E-01  6.85E-01  6.80E-01  6.60E-01
 6.90E-01  6.65E-01  6.75E-01  6.80E-01  6.60E-01  6.90E-01  6.40E-01
32            3.80E-06  9.60E-06 15.95E-06  21.5E-06  26.3E-06  31.9E-06  37.0E-06
 42.2E-06  47.9E-06  53.0E-06  58.5E-06  63.5E-06  69.0E-06  75.0E-06  79.5E-06
 84.5E-06  89.5E-06  95.0E-06 10.05E-05 10.50E-05 11.05E-05 11.55E-05 12.05E-06
12.55E-05 13.10E-05 13.65E-05 14.15E-05 14.70E-05 15.25E-05 15.75E-05 16.40E-05
17.25E-05
MILLER BOX M VNRAT VS TPRI DELT=.2US TPMAX=180US
R=.615M A=.0254M D=.0797M C=1479.55M/SEC 4/24/67
MILLER BOX M VNMAIN VS TPRI DELT=.2U TPMAX=180US
R=.615M A=.0254M D=.0797M C=1479.55M/SEC 4/24/67
MILLER BOX M VNCOR VS TPRI DELT=.2US TPMAX=180US
R=.615M A=.0254M D=.0797M C=1479.55M/SEC 4/24/67
GATEIN  NORM AMPRAT VS TPRI CAWN = 1.0C 5/5/67
```

414

INITIAL DISTRIBUTION LIST

		No. Copies
1.	Defense Documentation Center Cameron Station Alexandria, Virginia 22314	20
2.	Library Naval Postgraduate School Monterey, California 93940	2
3.	Anti-Submarine Warfare Systems Projects Office Washington, D. C. 20360	1
4.	Commander Naval Ships Systems Command Headquarters Washington, D. C. 20360	1
5.	Commander Naval Ordnance Systems Command Headquarters Washington, D. C. 20360	1
6.	Professor Herman Medwin Department of Physics Naval Postgraduate School Monterey, California 93940	1
7.	Professor Alan B. Coppens Department of Physics Naval Postgraduate School Monterey, California 93940	7
8.	LT Alan C. Miller Naval Weapons Station Yorktown, Virginia 23491	1
9.	LT George F. Wendt River Patrol Section 514 APO San Francisco, California 96627	1

UNCLASSIFIED

Security Classification

DOCUMENT CONTROL DATA - R&D

(Security classification of title, body of abstract and indexing annotation must be entered when the overall report is classified)

1. ORIGINATING ACTIVITY (Corporate author) Naval Postgraduate School, Monterey, California	2a. REPORT SECURITY CLASSIFICATION Unclassified	
	2b. GROUP NA	
3. REPORT TITLE Propagation of Two Simple Acoustic Transients in an Isovelocity Layer with Perfectly-Reflecting Boundaries		
4. DESCRIPTIVE NOTES (Type of report and inclusive dates) Thesis		
5. AUTHOR(S) (Last name, first name, initial) MILLER, Alan C., LT, USN; WENDT, George F., LT, USN		
6. REPORT DATE June 1967	7a. TOTAL NO. OF PAGES 117	7b. NO. OF REFS 19
8a. CONTRACT OR GRANT NO.	9a. ORIGINATOR'S REPORT NUMBER(S) NA	
b. PROJECT NO. NA		
c.	9b. OTHER REPORT NO(S) (Any other numbers that may be assigned this report) None	
d.		
10. AVAILABILITY/LIMITATION NOTICES [redacted]		
11. SUPPLEMENTARY NOTES None	12. SPONSORING MILITARY ACTIVITY Naval Ships Systems Command	

13. ABSTRACT

The propagation of simple acoustic transients in an isovelocity water layer was investigated for the purpose of studying a relationship between the propagation of transients in ducts and in layers. The Laplace transform method was used to obtain approximate solutions for the acoustic pressure, particle velocity, and particle displacement resulting from a step-function input in velocity and the particle velocity resulting from a gated sine-wave input in velocity. Computer programs were written to evaluate and graph the resulting waveforms. The waveforms resulting from step-function and gated sine-wave inputs in velocity were observed and compared with the predicted waveforms. With the use of Mylar transducers, good correlation was obtained in the region of validity of the theoretical solutions. It was found that previously published solutions for the propagation of transients in ducts became the leading terms of the associated solutions for the layer.

DD FORM 1 JAN 64 1473

UNCLASSIFIED

Security Classification

14. KEY WORDS	LINK A		LINK B		LINK C	
	ROLE	WT	ROLE	WT	ROLE	WT
Acoustic Transients						
Isovelocity Layer						
Mylar Transducers						
Lommel Function						
Laplace Transform						
Perfectly-Reflecting Boundaries						
Radially Symmetric Propagation						